



**HAL**  
open science

## **Early Triassic environmental dynamics and microbial development during the Smithian–Spathian transition (Lower Weber Canyon, Utah, USA).**

Anne-Sabine Grosjean, Emmanuelle Vennin, Nicolas Olivier, Gwénaél Caravaca, Christophe Thomazo, Emmanuel Fara, Gilles Escarguel, Kevin G. Bylund, James F. Jenks, Daniel A. Stephen, et al.

### ► To cite this version:

Anne-Sabine Grosjean, Emmanuelle Vennin, Nicolas Olivier, Gwénaél Caravaca, Christophe Thomazo, et al.. Early Triassic environmental dynamics and microbial development during the Smithian–Spathian transition (Lower Weber Canyon, Utah, USA).. *Sedimentary Geology*, 2018, 363, pp.136-151. 10.1016/j.sedgeo.2017.11.009 . hal-01659686

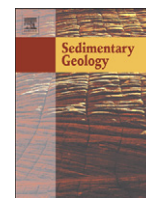
**HAL Id: hal-01659686**

**<https://hal.science/hal-01659686>**

Submitted on 9 Oct 2019

**HAL** is a multi-disciplinary open access archive for the deposit and dissemination of scientific research documents, whether they are published or not. The documents may come from teaching and research institutions in France or abroad, or from public or private research centers.

L'archive ouverte pluridisciplinaire **HAL**, est destinée au dépôt et à la diffusion de documents scientifiques de niveau recherche, publiés ou non, émanant des établissements d'enseignement et de recherche français ou étrangers, des laboratoires publics ou privés.



## Early Triassic environmental dynamics and microbial development during the Smithian–Spathian transition (Lower Weber Canyon, Utah, USA)



Anne-Sabine Grosjean<sup>a,b,\*</sup>, Emmanuelle Vennin<sup>a</sup>, Nicolas Olivier<sup>c</sup>, Gwénaél Caravaca<sup>a</sup>, Christophe Thomazo<sup>a</sup>, Emmanuel Fara<sup>a</sup>, Gilles Escarguel<sup>d</sup>, Kevin G. Bylund<sup>e</sup>, James F. Jenks<sup>f</sup>, Daniel A. Stephen<sup>g</sup>, Arnaud Brayard<sup>a</sup>

<sup>a</sup> Laboratoire Biogéosciences, UMR 6282, CNRS, Université Bourgogne Franche-Comté, 6 boulevard Gabriel, 21000 Dijon, France

<sup>b</sup> Laboratoire Magmas et Volcans, UMR 6524, CNRS, Université de Lyon, UJM-Saint-Etienne, UCA, IRD, 23 rue Dr Paul Michelon, 42023 Saint-Etienne, France

<sup>c</sup> Laboratoire Magmas et Volcans, CNRS, Université Clermont Auvergne, F-63000 Clermont-Ferrand, France

<sup>d</sup> Laboratoire d'Ecologie des Hydrosystèmes Naturels et Anthropisés, UMR 5023, CNRS, Université de Lyon, 3-6 rue Raphaël Dubois, 69622, Villeurbanne Cedex, France

<sup>e</sup> 140 South 700 East, Spanish Fork, UT 84660, USA

<sup>f</sup> 1134 Johnson Ridge Lane, West Jordan, UT 84084, USA

<sup>g</sup> Department of Earth Sciences, Utah Valley University, 800 West University Parkway, Orem, UT 84058, USA

### ARTICLE INFO

#### Article history:

Received 5 September 2017

Received in revised form 9 November 2017

Accepted 10 November 2017

Available online 22 November 2017

Editor: Dr. B. Jones

#### Keywords:

Early Triassic

Microbial deposits

MISS

Depositional environments

Smithian–Spathian transition

Western USA basin

### ABSTRACT

The Early Triassic biotic recovery following the end-Permian mass extinction is well documented in the Smithian–Spathian Thaynes Group of the western USA basin. This sedimentary succession is commonly interpreted as recording harsh conditions of various shallow marine environments where microbial structures flourished. However, recent studies questioned the relevance of the classical view of long-lasting deleterious post-crisis conditions and suggested a rapid diversification of some marine ecosystems during the Early Triassic. Using field and microfacies analyses, we investigate a well-preserved Early Triassic marine sedimentary succession in Lower Weber Canyon (Utah, USA). The identification of microbial structures and their depositional settings provide insights on factors controlling their morphologies and distribution. The Lower Weber Canyon sediments record the vertical evolution of depositional environments from a middle Smithian microbial and dolosiliclastic peritidal system to a late Smithian–early Spathian bioclastic, muddy mid ramp. The microbial deposits are interpreted as Microbially Induced Sedimentary Structures (MISS) that developed either (1) in a subtidal mid ramp where microbial wrinkles and chips are associated with megaripples characterizing hydrodynamic conditions of lower flow regime, or (2) in protected areas of inter- to subtidal inner ramp where they formed laminae and domal structures. Integrated with other published data, our investigations highlight that the distribution of these microbial structures was influenced by the combined effects of bathymetry, hydrodynamic conditions, lithology of the substrat physico-chemical characteristics of the depositional environment and by the regional relative sea-level fluctuations. Thus, we suggest that local environmental factors and basin dynamics primarily controlled the modalities of microbial development and preservation during the Early Triassic in the western USA basin.

© 2017 Elsevier B.V. All rights reserved.

### 1. Introduction

Following the end-Permian mass extinction, the Early Triassic recovery is generally associated with persistent or recurrent deleterious conditions such as anoxia, ocean acidification, unstable productivity and climate warming (Galfetti et al., 2007; Sun et al., 2012; Grasby et al., 2013). The post-crisis interval has notably been characterized by a “reef gap” (Flügel, 2002) with typical Permian metazoan reef-building organisms replaced by various microbial-dominated deposits.

Early Triassic microbial deposits are thus commonly described as “anachronistic facies” indicative of prolonged environmental stresses due to their similarities with some Precambrian and Cambrian facies (Baud et al., 1997, 2007; Pruss et al., 2004; Woods, 2014). Nevertheless, recent works highlighted that microbial deposits are sometimes associated with sponges and bivalves forming bioconstructions of different structures and sizes (Szulc, 2007; Brayard et al., 2011; Marengo et al., 2012), as well as with various inhabitants such as ostracods and gastropods for which they would have represented a potential refuge or food resource in the crisis aftermath (Forel et al., 2013; Brayard et al., 2015). Such consortia, as well as recent findings of diversified biotas, suggest that some settings were favourable to a rapid recovery after the end-Permian mass extinction (Brayard et al., 2015, 2017).

\* Corresponding author at: Laboratoire Biogéosciences, UMR 6282, CNRS, Université Bourgogne Franche-Comté, 6 boulevard Gabriel, 21000 Dijon, France.

E-mail address: [anne.sabine.grosjean@univ-st-etienne.fr](mailto:anne.sabine.grosjean@univ-st-etienne.fr) (A.-S. Grosjean).

Nevertheless, Early Triassic environmental conditions remain highly debated by the scientific community, which multiplies approaches (e.g., geochemistry, paleontology, sedimentology) and proxies to decipher local and regional environmental factors that influenced the biotic recovery. In some instances, these studies led to better identify the development of microbial deposits in some places (Payne et al., 2006; Kershaw et al., 2010; Vennin et al., 2015; Bagherpour et al., 2017; Tang et al., 2017).

Specific studies on Early Triassic microbial deposits mainly focus on microbialites, i.e., “organosedimentary deposits that have accreted as the result of a benthic microbial community trapping and binding detrital sediment and/or forming the locus of mineral precipitation” (Burne and Moore, 1987, p. 241–242). Early Triassic microbialites are observed in a wide range of depositional environments from platform interior to deep water settings (Baud et al., 2007; Woods and Baud, 2008; Kershaw et al., 2012; Mata and Bottjer, 2012; Vennin et al., 2015; Bagherpour et al., 2017). By contrast, Microbially Induced Sedimentary Structures (MISS; Noffke et al., 2001), i.e., benthic microbial communities inducing biostabilization of the substrate without direct carbonate precipitation (Noffke and Awramik, 2013), are more rarely described from Early Triassic exposures, and they mostly correspond to Spathian shallow peritidal environments (e.g., Pruss et al., 2004; Mata and Bottjer, 2009). Here, we study the sedimentary succession of the Lower Weber Canyon (LWC) section in northern Utah, USA (Fig. 1) that records well-preserved MISS during a long-time interval from the Smithian up to their cessation just before the Smithian/Spathian Boundary (SSB). The LWC section is characterized by the evolution of sedimentation from dolosiliciclastic- to carbonate-dominated deposits. The aims of this study are: (i) the reconstruction of paleoenvironments and factors influencing the transition from dolosiliciclastic to carbonate-dominated sedimentation, (ii) the characterization of MISS within their stratigraphic and sequential framework, and (iii) the identification of controlling factors acting on the presence of MISS during the Smithian and their cessation.

## 2. Geological setting

During the Permian-Triassic transition, the Sonoma orogeny led to the formation of the western USA basin, named the Sonoma Foreland Basin (SFB), located at a near-equatorial position on the western Pangea margin (Fig. 1A; Burchfiel and Davis, 1975; Ingersoll, 2008; Dickinson, 2013). This sedimentary basin mainly extends from the modern states of Idaho and Wyoming to Utah and eastern Nevada. In this area, the Early Triassic sea-level displayed a long-term transgression with a main NW–SE orientation (Fig. 1B; Paull and Paull, 1993; Lucas et al., 2007; Brayard et al., 2013; Olivier et al., 2014) within a complex basin-floor paleotopography resulting from differential subsidence (Blakey, 1977; Caravaca et al., 2017a). This Smithian regional sea-level rise corresponds to the transgressive semi-cycle of the second third-order transgressive-regressive (T-R) sequence recorded in the SFB (Haq et al., 1987; Paull and Paull, 1993; Embry, 1997). The late Smithian ammonoid *Anasibirites* bearing beds record the maximum flooding at the basin scale, before a regressive trend starting in the early Spathian (Collinson and Hasenmuller, 1978; Carr and Paull, 1983; Paull and Paull, 1993; Lucas et al., 2007; Brayard et al., 2013; Jattiot et al., 2017).

In this context, the resulting Early Triassic sedimentary succession is spatially heterogeneous, ranging from continental terrigenous conglomerates and sandstones of the Moenkopi Group to mixed terrigenous and marine carbonates of the Thaynes Group (Lucas et al., 2007). The latter stratigraphic unit typically displays shale-limestone alternations of a shallow marine platform (McKee, 1954; Collinson et al., 1976). Following the NW–SE transgression across the SFB (Fig. 1B), these marine deposits interfinger with and overlap the Moenkopi Group southward (e.g., Lucas et al., 2007; Caravaca et al., 2017a). From southern Idaho to southern Utah, the Early Triassic rocks overlies unconformably various middle Permian rocks highlighting the major

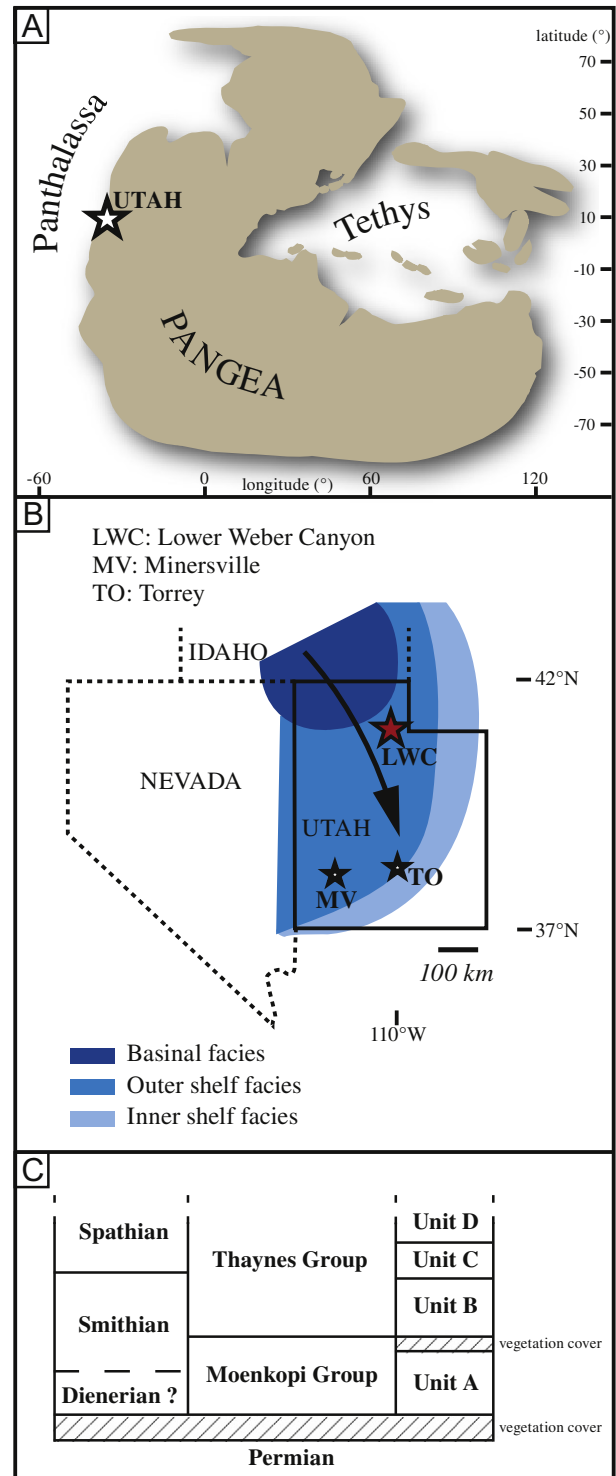


**Fig. 1.** (A) Early Triassic location of the western USA basin (modified from Brayard et al., 2013). (B) Illustration of the NW–SE transgression recorded in the Smithian sedimentary successions of Utah (modified from Lucas et al., 2007; Brayard et al., 2013). Lower Weber Canyon (this work), Mineral Mountains (Vennin et al., 2015) and Torrey (Olivier et al., 2016) sections are indicated. (C) Simplified stratigraphic subdivision of the Early Triassic sedimentary succession at the LWC section.

regional stratigraphic and sedimentary hiatus of the Permian – Triassic transition (Newell, 1948; Clark, 1957; Hose and Repenning, 1959; Collinson et al., 1976; Goodspeed and Lucas, 2007). Recent biostratigraphical studies on bivalve and ammonoid occurrences led to the calibration of the Early Triassic sedimentary succession in central and southern Utah from the Dienerian to early Spathian (Brayard

et al., 2013; Hofmann et al., 2014). A robust middle to late Smithian biostratigraphic framework based on ammonoids is also available for most parts of the basin (Brayard et al., 2009, 2013; Jattiot et al., 2016, 2017). Various Smithian and Spathian microbial deposits have already been reported within the SFB (Schubert and Bottjer, 1992; Pruss et al., 2004; Mata and Bottjer, 2009, 2011; Vennin et al., 2015; Olivier et al., 2016), but to our knowledge, no Smithian MISS. Older MISS were also recently reported from the Griesbachian (?) of southern Idaho and Montana (Wimer, 2015), but their exact ages need to be confirmed.

### 3. The Lower Weber Canyon section

The Weber Canyon studied portion takes its usage name from the geological community (Smith, 1969 and reference therein). This historical name do not corresponds to the modern day geographical map name which is 'Upper Weber Canyon'. To avoid confusion among the geological community, we have chosen to use the established usage name 'Lower Weber Canyon'. The section is located in the north-eastern part of the SFB (Fig. 1B). It is divided into two distant successions separated by the Interstate Highway 84 along the Weber River. These two successions are correlated based on the occurrence of the *Anasibirites* beds on both sides of the road (Fig. 2). Overall, the complete Early Triassic sedimentary succession observed along LWC consists of 4 lithostratigraphic units (Unit A to D; Fig. 1C). The base of the studied section is unclear due to a 60 m thick vegetation cover at the transition between Permian rocks and Unit A. The upper Permian deposits are also markedly faulted as indicated by changes in the stratigraphic inclination and the presences of fault structures. Additionally, a sedimentary gap is likely between Permian rocks and Unit A. The Unit A is characterized by 40 m of well-preserved red beds of the Moenkopi Group, described as

continental to tidal flat environments (Dienerian–Smithian?; Smith, 1969). These red beds are not described in this work. They are overlain by a 60 m-thick vegetation-covered interval followed by 188 m of mixed dolosiliciclastic, carbonate and marl sediments belonging to the Thaynes Group (Smith, 1969) that correspond to Units B, C and D (Figs. 1C and 2). Unit B (111 m-thick) comprises dolosiliciclastic sediments with MISS occurrences and intercalated cm- to dm-thick calcarenitic bioclastic levels (Fig. 3A). The co-occurrence of ammonoid genera *Juvenites*, *Paranannites*, *Owenites* and *Meekoceras* (noted as *Mee.* in Fig. 3A) indicates that Unit B was deposited during the middle Smithian (*Owenites* beds in Brayard et al., 2013; UAZ<sub>4</sub> in Jattiot et al., 2017). Unit C is composed of 36 m of silty and carbonate layers in marl dominated sediments. Its base contains more carbonate beds than the subsequent part of Unit C and corresponds to the *Anasibirites* beds of late Smithian age (noted as *Ana.* in Figs. 2 and 3A; Brayard et al., 2013). Unit D (41 m-thick) corresponds bioclastic-dominated deposits interbedded in mudstones and is Spathian in age (noted layered limestones in Fig. 3A; Smith, 1969). At the top of the section, Unit D records a return to a dolosiliciclastic-dominated sedimentation without microbial deposits.

### 4. Facies associations and depositional environments

Macroscopic and microscopic observations on 219 thin sections have been performed for facies identification. Nine facies associations (F1 to F9) have been recognized and interpreted in terms of flow regime and tidal zonation (supratidal, intertidal and subtidal). They have been then integrated in four depositional environments that are distributed along a ramp system from (1) microbial dolosiliciclastic peritidal ramp, (2) tide-influenced bioclastic mid ramp, (3) storm-dominated

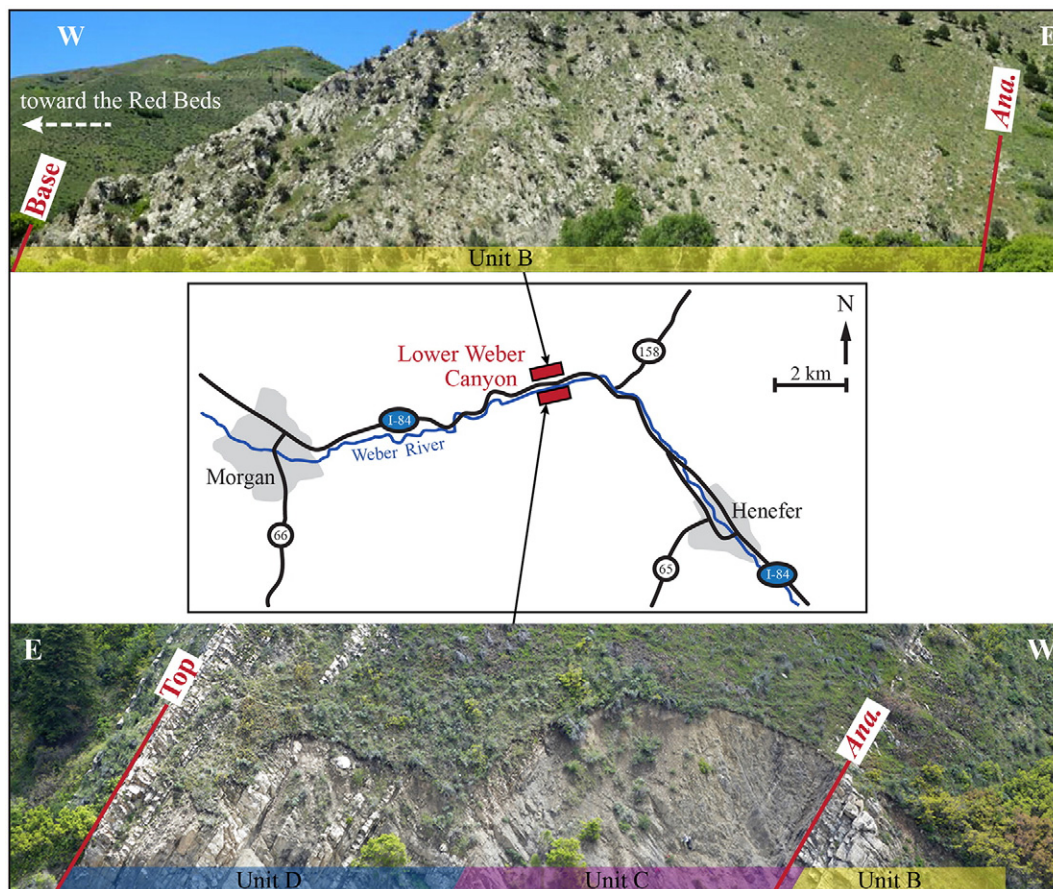
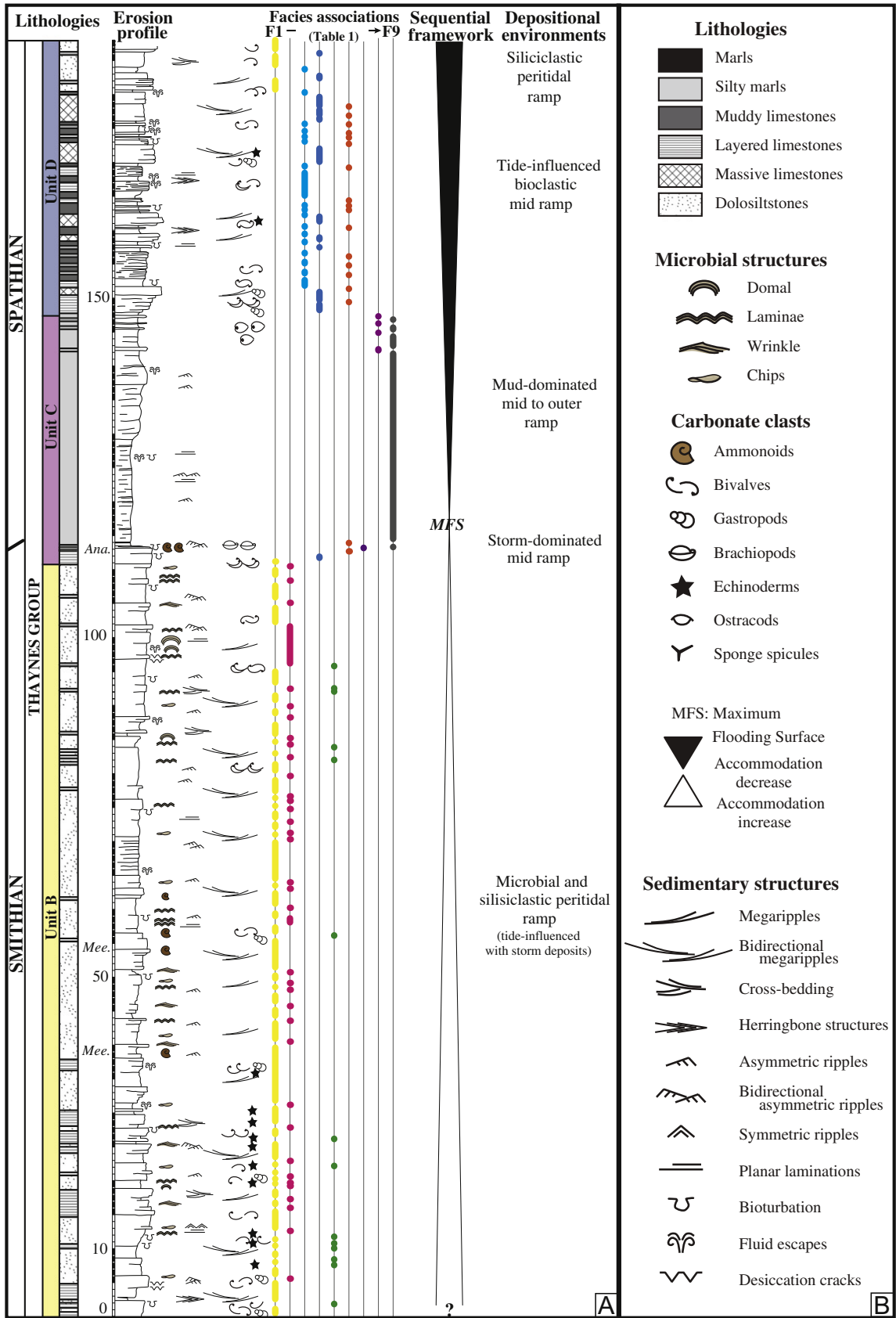


Fig. 2. Panoramas of the Lower Weber Canyon section separated by the Interstate Highway 84 and the Weber River. *Anasibirites* beds (*Ana.*) provide a precise correlation between the two parts of the section. The distribution of described lithostratigraphic units B, C and D are also indicated.



**Fig. 3.** (A) Synthetic sedimentary succession of the Lower Weber Canyon section with lithostratigraphic units B, C and D (Fig. 2; Unit A is not described in this work). *Meekoceras* and *Anasibirites* ammonoid beds (*Mee.* and *Ana.* respectively), compositional characteristics of facies associations and depositional environments, as well as the regional sequential framework are indicated. (B) Legend for Figs. 3A and 8.

**Table 1**

Classification of the nine facies associations determined along the LWC section with their diagnostic compositions and features, their stratal pattern and their corresponding depositional environments.

Facies associations	Diagnostic features	Other components	Sedimentary structures	Stratal pattern	Flow regime and zonation	Depositional environment
F1: dolosiltstones to bioclastic grainstones/calcarenites	(a) Well-sorted quartz and dolomite (up to 50%) silts in a sparitic cement	Rare muscovite and glauconite. Oxides and sulphurs are also present. Rare bioclastes (bivalves, echinoderms, phosphate remains)	Flat uni- and bidirectional megaripples, upper plane bed planar laminations, symmetric wave and asymmetric current ripples, trough cross stratifications, mud drapes, fluid escape, desiccation cracks. Locally presenting clast size sorting (silts vs fine silts). Rare to moderate bioturbation	Decimetre to metre thick beds; and metre to plurimetre wide	Lower part to upper part of the lower flow regime, inter to subtidal	Microbial and/or siliciclastic peritidal ramp
	(b) Highly fragmented thin-shelled bivalves in a dolosilty matrix to a sparitic cement	Gastropods, echinoderms and phosphate remains	Flat uni- and bidirectional megaripples, asymmetric current ripples, trough cross stratifications, mud drapes, fluid escape. Rare to moderate bioturbation	Decimetre to metre thick beds; and metre to plurimetre wide	Lower part to upper part of the lower flow regime, inter to subtidal	
	(c) Highly fragmented echinoderms in a dolosilty matrix to a sparitic cement	Bivalves, gastropods and phosphate remains	Flat uni- and bidirectional megaripples, asymmetric current ripples. Rare to moderate bioturbation	Decimetre thick in metre wide	Upper part of the lower flow regime, subtidal	
F2: Microbial structures	(a) Multi-layered dark organic laminae forming small domal structures of few centimetre thick in a dolosilty matrix	Rare bivalves	Truncating erosion surfaces, toplap on the edge of domes, fluid escape, rare bioturbation	Centimetre to decimetre thick beds	Lower part of the lower flow regime, intertidal	
	(b) Undulated dark organic laminations, more or less continuous in a dolosilty matrix. Laminae: laterally continuous, few microns-thick sometime stack into millimetric levels. Wrinkle: laminae of various thickness from few to undreds microns capping sedimentary structures	Rare bivalves, echinoderms and phosphate remains	Fluid escape, rare bioturbation, desiccation cracks	Centimetre to decimetre thick beds at the base or at the top of megaripples; or pluridecietre to metre massive wide units	Lower part of the lower flow regime, inter to subtidal	
	(c) Chips: dense or peloidal clotted patches; or disrupted laminae in a dolosilty matrix	Rare bivalves, echinoderms and phosphate remains	Fluid escape, rare bioturbation	Centimetre thick beds on top of megaripples	Upper part of the lower flow regime, subtidal	
F3: Sponge and ostracod mudstones- wackestones	Dominated by disarticulated ostracod shells and sponge spicules. Micritic to microsparitic matrix	Rare to common bivalves. Rare detritic levels/laminae	Planar laminations, asymmetric current ripples, herringbones, flaser bedding, rare bioturbation	Centimetre to pluridecimetre thick	Lower part of the lower flow regime and decantation, inter to subtidal	Tide-influenced bioclastic mid ramp

F4: Bivalve-rich packstones	Dominated by the association of thin and thick disarticulated to fragmented shells of bivalves. Micritic to microsparitic matrix	Common gastropods, rare echinoderm and serpulidae clasts. Rare to moderate detritism	Uni- and bidirectional megaripples, mud drapes, fluid escape, rare bioturbation	Decimetre to pluridecimetre thick beds; and metre to plurimetre wide	Upper part of the lower flow regime, inter to subtidal	
F5: Bioclastic packstones to calcarenites	(a) Highly fragmented thin-shelled bivalves. Dolosilty matrix to sparitic cement	Rare gastropods with micritic filling, echinoderms, phosphate remains, ostracods and ammonoids	Rare bioturbation	Sheet-like or lenticular centimetre to decimetre thick beds with erosive or sharp bases	Upper flow regime, subtidal	
	(b) Disarticulated thin- and thick-shelled bivalves presenting micritic and/or sparitic filling. Dolosilty matrix to sparitic cement	Gasteropods, echinoderms, phosphate remains	Normal grading, concave up orientation of shells, rare bioturbation	Sheet-like pluricentimetre thick beds with erosive or sharp bases	Upper flow regime, subtidal	
	(c) Highly fragmented echinoderms. Dolosilty matrix to sparitic cement	Common bivalves, rare gastropods and phosphate remains	Asymmetric ripples, fluid escape, rare bioturbation	Sheet-like centimetre to decimetre thick beds with erosive or sharp bases	Upper flow regime, subtidal	
F6: Bivalve and ammonoid packstones/grainstone to floatstones	(a) Bivalve packstone/grainstone. Dominated by the association of thin and thick disarticulated shells of bivalves. Micritic matrix to sparitic cement	Common gastropods and ostracods, rare phosphate remains, echinoderms and serpulidae, frequent to rare detritism. Sometime presenting progressive vertical evolution from bioclastic calcarenite to wackestone	Umbrella structures, sometime with convexe up to concave up vertical evolution of shell orientation	Sheet-like or lenticular centimetre to decimetre thick beds with erosive or sharp bases	Upper flow regime	Storm-dominated mid ramp
	(b) Fragmented large-shelled bivalve floatstone. Shells have a coarsely prismatic structure. Micritic to microdolomitic matrix	Rare ostracod shells, common sponge spicules, common detritism	Valve orientation parallel to the planar laminations, bidirectional ripples	Decimetre tabular bed, platy parting	Upper to lower flow regime	
	(c) Ammonoid floatstone in a micritic to peloidal matrix	Bivalves, ostracods, sponge spicules, rare gastropods, moderate detritism	Clast orientation parallel to the stratification	Massive decimetric bed	Upper flow regime	
F7: Peloid and brachiopod grainstones to mudstones	Progressive vertical evolution from peloidal grainstone, brachiopod-gastropod grainstone to wackestone/mudstone	Rare ammonoids, bivalves and ostracods, common to rare detritism	Planar laminations, moderate bioturbation	Decimetre to pluridecimetre thick beds with sharp bases	Upper to lower flow regime	
F8: Thick bivalve floatstones	Articulated to disarticulated thick-shelled bivalves. Micritic to microsparitic matrix	Rare ostracods and gastropods, rare detritism	Massive	Centrimetric levels	Lower flow regime and/or decantation	Mud-dominated mid to outer ramp
F9: Mudstones	(a) Laminated micritic to microdolomitic muds with rare fine dolosilty layers	Rare muscovite, rare bivalves	Planar laminations, asymmetric current ripples, rare bioturbation		Upper to lower flow regime	
	(b) Black marls		Planar laminations	Centimetric to decimetric intervals	Lower flow regime and decantation	

mid ramp, to (4) mud-dominated mid to outer ramp. In dolosiliclastic sediments, the recognition of MISS is commonly based on indirect signatures (i.e., sedimentary surface textures). In this study, we followed the macro- and micro-criteria of Davies et al.'s (2016) classification, which was established by (i) comparison with modern MISS, (ii) identification of hydrodynamic conditions during their deposition, and (iii) textural evidence of grain stabilization when possible. Facies associations are synthesized in Table 1 and illustrated in Figs. 4–7. A depositional model is proposed for the studied LWC sedimentary succession based on the reconstructed environments, their sedimentary structures and their litho- and bioclastic characteristics (Fig. 8).

#### 4.1. Microbial and/or siliciclastic peritidal ramp

##### 4.1.1. Description

This depositional environment is dominated by the dolosiltstone to bioclastic calcarenitic facies association (F1) that represents the frame of Unit B and is associated with the microbial facies association F2. F1 also corresponds to upper Unit D. F1 is organized into dm-thick beds stacked in metre to plurimetre wide units. It is characterized by megaripples (Fig. 4A) that commonly display bidirectional cross-bedded structures and mud drapes (Fig. 4B). F1 is subdivided into three subfacies associations. F1a consists of carbonate-cemented dolosiltstones where quartz and dolomite are about 50–60% and 10–30% of the grain composition respectively. Rare bioclasts (bivalves, echinoderm plates) and phosphate remains are observed, as well as accessory minerals (muscovite, glauconite, pyrite, undetermined oxides), representing less than 5% of the grains. F1b presents an abundance of highly fragmented bivalve shells in a dolosilty matrix to a sparitic cement (Fig. 4C). The grain composition in quartz and dolomite is the same than F1a (Fig. 4D). F1c consists of frequent to abundant, highly fragmented echinoderm plates also observed in a dolosilty matrix to a sparitic cement (Fig. 4E). Clasts of echinoderms are well sorted and well rounded. Facies association F2 is composed of dark organic undulated structures trapping dolosilty grains presenting the same composition as F1a. It is observed capping the top or the base of some flat megaripples (Fig. 4F). It also appears as massive decimetric to metric beds (Fig. 4G) that present desiccation cracks at their top (Fig. 4H). F2 is also subdivided into three subfacies associations. F2a corresponds to multi-layered, undulated and commonly discontinuous laminae in the dolosilty matrix locally inducing domes of a few cm-thick in diameter (Fig. 5A and B). F2a is observed in centrimetric to decimetric levels embedded in the dolosiliclastic sedimentation, and is better expressed in the massive upper part of Unit B (Fig. 3A). F2b displays various textures (planar, wavy or bulbous) at the macroscale along the erosion profile (Fig. 5C, D and E). At micro-scale, it is characterized by more or less continuous laminations ('laminae' and 'wrinkle'). F2b is observed at the base or at the top of the megaripples or within massive beds. Laminae are sometime fused in tens to hundred  $\mu\text{m}$ -thick laminae (Fig. 5F). Wrinkle structures are preserved on top of megaripples. The microfabric is composed of dark organic layers draping ripples and cross-bedded sedimentary structures (Fig. 5G). F2c is only preserved in megaripples. Its microfabric is composed of dense or peloidal clotted patches of organic material named 'chips' (Fig. 5H).

##### 4.1.2. Interpretation

The recurrence of megaripples that commonly present bidirectional laminations and mud/fine silt drapes suggests the deposition of the dolosiltstones and bioclastic grainstones/calcarenites of F1 under moderate hydrodynamic conditions (lower to upper part of the lower flow regime) with a tidal influence in a peritidal domain from inter- to shallow subtidal zones (Johnson and Baldwin, 1996; Nichols, 2009). The concentrations of bivalves and echinoderms (F1b and F1c) in dolosiliclastic megaripples suggest their remobilization during megaripple deposition. The colonization of quartz-sand dominated sediments by microbial biofilms is recurrent in modern and ancient

peritidal clastic settings (Gerdes, 2010; Noffke, 2010). The preservation of F2 at the top and at the base of some megaripples suggests that they were deposited in the same environment as F1, where desiccation cracks mark periods of subaerial exposure in the intertidal zone (Burchette and Wright, 1992; Flügel, 2004). In modern environments, microbial features are commonly associated with megaripples of mid ramp, but are also particularly well-preserved in the inner peritidal domain where they contribute to the biostabilization of the siliciclastic substrate (Gerdes et al., 2000; Cuadrado et al., 2011, 2014; Noffke and Awramik, 2013). The preserved planar, undulated, wavy and bulbous laminae of F2a and F2b suggest that filament-dominated microbial mats acted on the preservation of sedimentary structures (Schieber, 1999; Werhmann et al., 2012). As no evidence of microbial-induced precipitation is observed, these structures are considered as MISS (Noffke et al., 2001; Noffke, 2010; Davies et al., 2016). The domal structure of F2a underlines a sufficient accommodation for a vertical binding of microbial mats (Noffke and Awramik, 2013). Alternatively, studies in recent peritidal settings suggest that such domal structures are commonly observed in quiet and protected zones and are supposed to form by trapped gases in voids or by vertical pushing due to gas pressure in flat microbial mats (Reineck et al., 1990; Gerdes et al., 1993; Gerdes and Krumbein, 1994; Bouton et al., 2016). The association of flat laminae with megaripples, as well as the replication of ripples by mats forming wrinkle structures, suggest the flourishing of F2b in more open zones and intermittent energy (Gerdes and Krumbein, 1994; Gerdes et al., 2000; Vennin et al., 2015; Bouton et al., 2016). In this peritidal domain, chips of F2c are considered as reworked clasts of biofilms. As they exhibit similar characteristics to F2b, they likely represent microbial mat or biofilm fragments remobilized by curling or fraying by waves and tidal currents (Pflüger and Gresse, 1996). They are interpreted as originating during "mechanical deformation of biologically stabilized surfaces" (Gerdes et al., 2000) in the upper part of the lower flow regime.

#### 4.2. Tide-influenced bioclastic mid ramp

##### 4.2.1. Description

This depositional environment is marked by a low siliciclastic supply and by shell accumulations. It is characterized by bioclastic facies association F4 embedded into the muddy facies association F3 during carbonate sedimentation of Unit D; and by F5 intercalated within the dolosiliclastic sedimentation of Unit B (Fig. 3A). Facies association F3 forms centimetre- to pluridecimetre-scale beds that commonly display planar and rare bidirectional structures. It appears in alternation with bioclastic facies associations F4 and F6 in Unit D (Figs. 3 and 6A). It consists of mudstones/wackestones containing common to frequent sponge spicules and ostracod shells in a micritic to microsparitic matrix (Fig. 6B). Bivalve-rich F4 is organized into dm-thick beds stacked into metre to plurimetre wide units in Unit D (Fig. 6A). It is characterized by flat uni- and bidirectional megaripples that commonly display mud drapes. F4 is a packstone that consists of disarticulated to fragmented, thin and thick-shelled bivalves without preferential orientation (Fig. 6C). Gastropods are also commonly observed and more rarely echinoderms, as well as a low siliciclastic content. F5 is intercalated within the dolosiliclastic sedimentation of Unit B as sheet-like or lenticular cm- to dm-thick beds that locally display erosive bases. It is represented by three subfacies associations of bioclastic calcarenites. F5a is characterized by highly fragmented, thin-shelled bivalves without preferential orientation that are associated with rare to common gastropods presenting micritic filling (Fig. 6D). F5b consists of thick and thin-shelled bivalves presenting micritic and/or sparitic filling. Shells are disarticulated (but not fragmented) and have a preferential concave up orientation (Fig. 6E). F5c is almost entirely composed of highly fragmented, well-sorted and moderately rounded echinoderms, commonly associated with bivalve and phosphate remains (Fig. 6F).

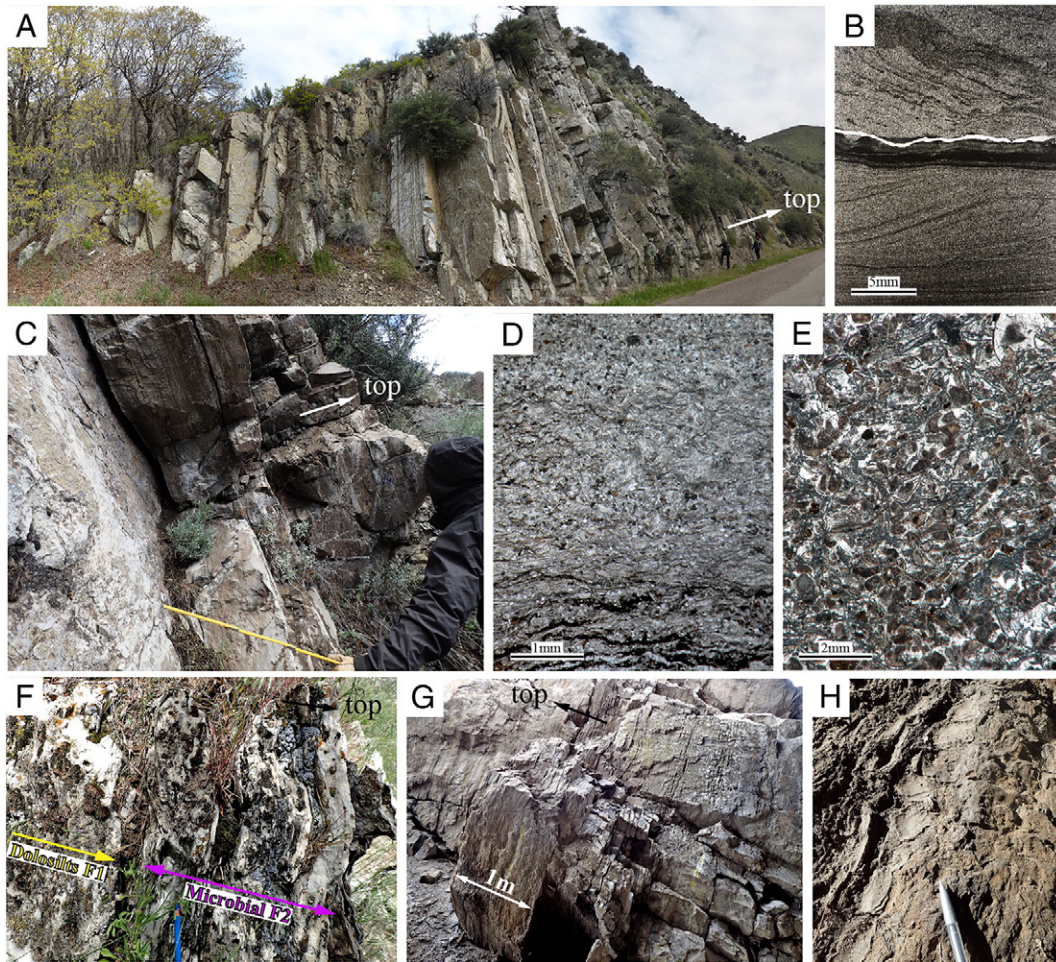


**Fig. 4.** Facies association illustrations of the peritidal depositional setting (Unit B). (A) Field view of dolosiltstones and bioclastic calcarenites/grainstones (F1) organized into megaripples. (B) Microphotograph of bidirectional ripples in F1a, separated by mud drapes. (C) Flat megaripples of calcarenitic F1b where shells of bivalves are embedded within the same dolosilt matrix as F1a. (D) Microscopic view of F1b; note the high fragmentation of shells by current activity. (E) Well-sorted and well-rounded echinoderms in F1c. (F) Top of a dolosilt megaripple capped by the microbial facies association F2b at the base of Unit B. (G) Organization of F2a into massive metric beds at the top of Unit B. (H) Desiccation cracks, associated with MISS, preserved at the top of massive beds. The top of the section is indicated on field views.

#### 4.2.2. Interpretation

The presence of uni- and bidirectional structures frequently preserved in bioclastic facies association F4 and in muddy F3 suggest a deposition under a lower flow hydrodynamic regime shallow-water depositional system with a tidal influence (Johnson and Baldwin, 1996; Nichols, 2009). F4 consists in well-defined accumulations of bioclasts that associate gastropods and echinoderms with the bivalve-dominated packstones. They are interpreted as shell concentrations (as defined by Kidwell et al., 1986). As F3 is associated with the bioclastic bodies of F4 (Unit D), it is interpreted as deposited in more protected areas in inter-megaripple position (Tucker, 1985). Moreover, the megaripples resulting from the bioclastic accumulations of F4, as well as the sheet-like and lenticular morphologies of F5 beds commonly underlined by erosive or sharp bases, indicate their deposition under moderate to high flow regime on the mid ramp (Wright and Burchette, 1996; Nichols, 2009). As facies association F5 appears as isolated sheet-like beds with sharp to erosive bases in the main dolosiliclastic sedimentation of Unit B, it is interpreted as storm washovers recording transport under upper flow regime events (Kidwell and Bosence, 1991; Fürsich and Oschmann, 1993) that commonly remobilize bivalves, gastropods (F5a and F5b) and echinoderms (F5c) from mid to inner domains of the ramp (Seilacher, 1982; Pruss et al., 2004). Such reworking is also supported by the micritic filling of gastropods (F5a) and partially of bivalves (F5b) that were likely deposited on the carbonate-dominated

mid ramp domain and then transported to the dolosiltstone-dominated inner domain of the ramp (Unit B). They are interpreted as storm-induced deposits (Aigner, 1985; Brechley and Harper, 1998) and highlight the recurrent remobilization of bioclasts by storm activity on the ramp (Tucker, 1985; Monaco, 2000; Pruss et al., 2004).

#### 4.3. Storm-dominated mid ramp

##### 4.3.1. Description

This domain is characterized by facies associations F6 and F7 (Fig. 3A). The bioclastic composition of F6 leads to the identification of three subfacies associations. F6a is intercalated into the bioclastic muds (F3) and megaripples of F4 in Unit D; while F6b, F6c and F7 mark the base of Unit C. F6a is mainly interbedded within the mud sedimentation of Unit D (F3) and more rarely integrated into bioclastic megaripples of facies association F4 (Fig. 3A). It corresponds to sheet-like or lenticular pluri-cm- to dm-thick beds presenting sharp or erosive bases. Bioclasts almost entirely consist of disarticulated thin or thick shells of bivalves with a packstone/grainstone texture, sometime forming umbrella structures, and commonly associated with gastropods and ostracods (Fig. 7A). More rarely, it is marked by the progressive evolution from bioclastic calcarenites to wackestones deposited on an undulated erosive base. F6b consists of a unique 50 cm-thick flatbed preserved at the base of Unit C. It is a floatstone characterized by

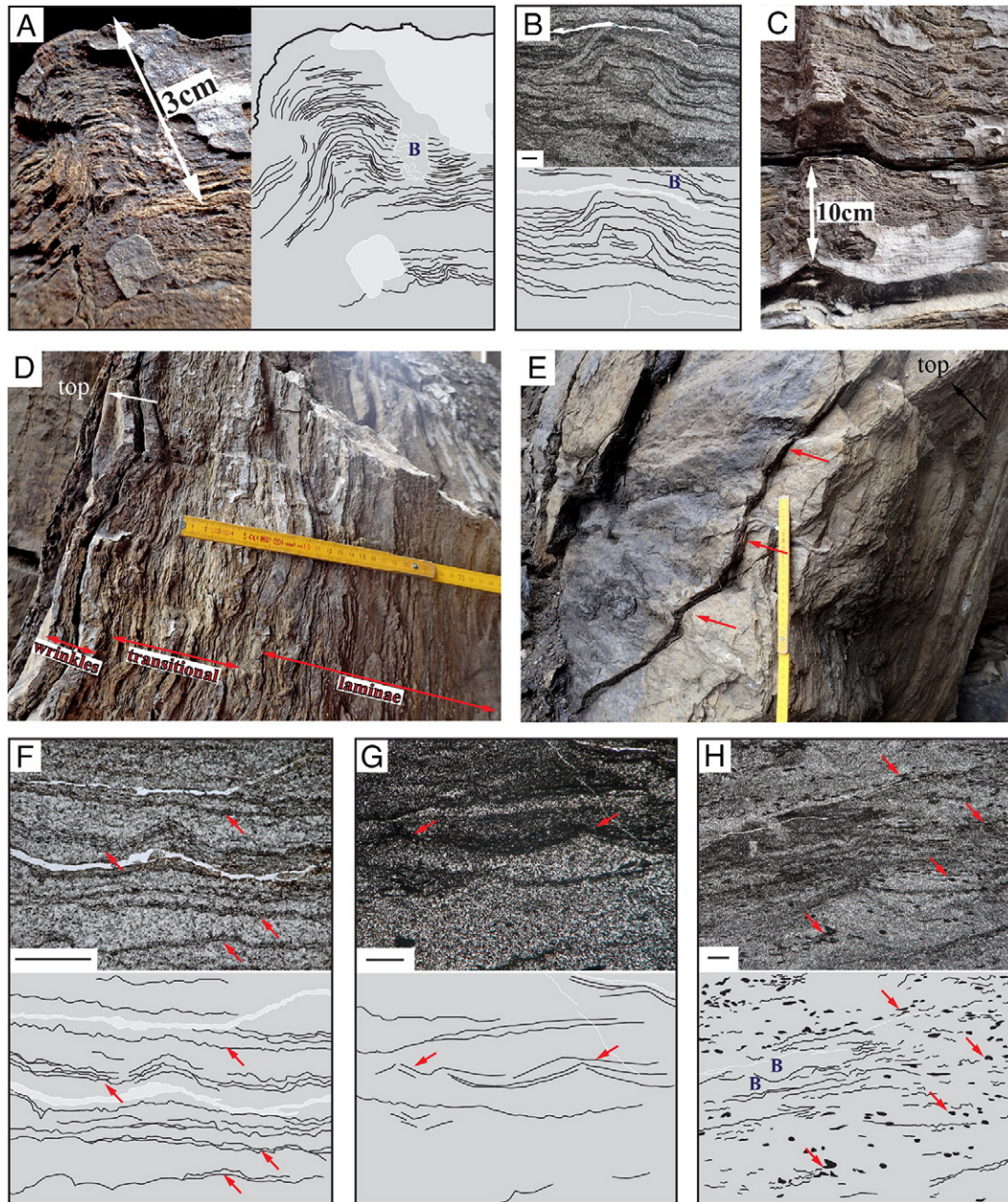


**Fig. 5.** Illustrations of the characteristic growth morphologies and microstructures of the microbial facies association F2 preserved in a dolosilty matrix in Unit B. (A) Field view of domal structures of F2a. (B) Microphotograph of dark and light alternations forming small domes (F2a) during dolosilty sedimentation. (C) Field view of irregular and undulated microbial laminae of F2b. (D) Vertical transition from laminae to wrinkles at the top of massive beds. (E) Upper surface of a bed illustrating the wavy structure of wrinkles (F2b). (F) Microphotograph of dark and light alternations stacked into relatively continuous laminae (F2b). (G) Microphotograph of wrinkle structures represented by microbial mat draping ripples. (H) Clotted texture of chips resulting from the disaggregation of microbial mats. (Scale bar of thin-section illustrations = 1 mm. B = bioturbations). The top of the section is indicated on field views.

large-sized bivalves and sponge spicules embedded in microdolomitic matrix (Fig. 7B). The shells are fragmented with a preferential horizontal position parallel to the stratification. F6c is characterized by ammonoids and bivalves floating in a micritic to peloidal matrix with a preferential orientation parallel to the elongation of the shells (Fig. 7C). Ammonoids and bivalves are of various sizes. Bivalves are disarticulated to fragmented, and ammonoid shells are complete to fragmented. F7 is composed of carbonate beds interbedded within black marls (F9b) at the base of Unit C (Fig. 7D). It exhibits a textural trend from a sharp base that vertically evolves from a peloidal grainstone, to a brachiopod/gastropod grainstone containing some ammonoids, and finally to a laminated mud (Fig. 7E).

#### 4.3.2. Interpretation

The deposition of peloid/brachiopod grainstones (F7) and bivalve-rich packstones (F6a), as well as the vertical evolution of their textures, argue for a deposition during storm events in open-wave domain of the mid ramp (Aigner, 1985; Fürsich and Oschmann, 1993). As F6a is observed intercalated within mud (F3) and bioclastic megaripples (F4) of Unit D, it is interpreted as incursions of 'proximal tempestites' superposed to the mid ramp setting as commonly observed in modern and ancient environments (Aigner, 1982; Seilacher, 1982; Tucker, 1985). As observed by Boyer et al. (2004), such bioclastic storm-induced deposits seem to be recurrent during the shallow marine sedimentation of the Early Triassic SFB. By contrast, the increase in micritic

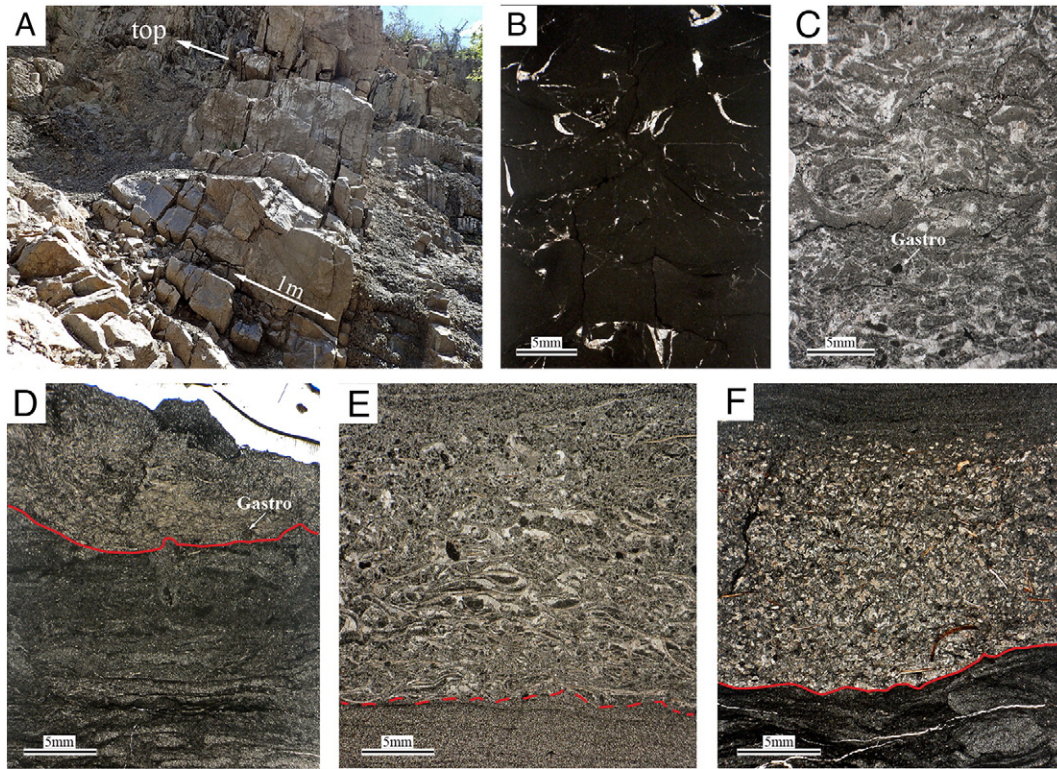


**Fig. 6.** Facies association illustrations of the bioclastic mid ramp setting. (A) Stacking pattern of the bioclastic mudstone/wackestone facies association F3 interbedded with the bioclastic packstone F4 (the top of the section is indicated on the picture). (B) Microscopic view of F3, rare shells of bivalves are preserved and embedded in a micritic matrix. (C) Microscopic characteristics of facies association F4; note that gastropod shells present micritic filling. (D) Microphotograph of an intercalation of bivalve-dominated F5a interpreted as storm events embedded into the microbial facies association F2; note the irregular erosional surface at the base of the bioclastic level. (E) Microphotograph of F5b presenting a sharp base in contact with F1. Shells of bivalves present a peculiar concave-up orientation, sometimes showing a geopetal filling. (F) Microphotograph of F5c intercalated within F2; note the upward decrease in echinoderm and phosphate clast size.

matrix in F6b and F6c, and the presence of ammonoids associated with brachiopods and peloids in F6c, suggests a deeper environment than the one proposed for F6a. Thus, F6b and F6c likely correspond to 'distal tempestites' deposited in an outer position on the mid ramp system (Burchette and Wright, 1992). The internal orientation of bioclasts parallel to the stratification suggests their deposition during high flow regime events such as storms (Aigner, 1985; Monaco, 2000) commonly observable in the offshore transition zone (Bridge and Demicco, 2008; Nichols, 2009). Finally, the accumulation of weakly fragmented shells of ammonoids and bivalves in a micritic matrix (F7) suggests local potential reworking without transport on the distal part of the mid ramp (Seilacher et al., 1985; Kidwell et al., 1986).

#### 4.4. Mud-dominated mid to outer ramp

##### 4.4.1. Description

The mud-dominated mid to outer ramp domain mainly corresponds to Unit C (Fig. 3A). It is composed of thick bivalve floatstones (F8) interbedded within fine deposits (F9). F8 is organized into well-defined centimetric levels within the muddy facies association F9. It is characterized by articulated or disarticulated (but not fragmented) thick bivalve shells floating in a micritic to microsparitic matrix (Fig. 7F). The articulated valves present a vertical to oblique orientation, while the disarticulated valves are preferably parallel to the stratification. Facies association F9a is organized into cm- to dm-thick well sorted fine-grained dolosiltstones interlayered with laminated micritic to microdolomitic muds (Fig. 7G). The dolosilt layers display a recurrence of planar laminations and current ripples that are underlined by millimetric layers of clay sometimes disrupted by fluid escapes and bioturbation. Facies association F9b is observed at the base of Unit C in

alternation with bioclastic facies associations F6b and F7. It is entirely composed of planar bedding black marls (Fig. 7D).

##### 4.4.2. Interpretation

The preservation of articulated shells in F8 argues for a shell accumulation with weak post-deposition hydraulic or biologic reworking (Kidwell et al., 1986). This suggests that shell assemblages mainly reflect the local life environment, possibly recording a rapid burial (Brett and Seilacher, 1991). F8 was likely deposited under low hydrodynamic regime and/or by decantation (Seilacher et al., 1985) in a distal part of the mid ramp. In the absence of bidirectional structures, the dominance of fine-grained sediments argues for the deposition of F9a and F9b under low hydrodynamic conditions in a distal mid to outer ramp setting below or close to the normal storm wave base (Burchette and Wright, 1992; Nichols, 2009). The intercalations of fine-dolosiliclastic layers in muddy F9a underline the exportation of sediments to the distal part of the ramp. The presence of asymmetric ripples indicates the action of currents during the deposition of these fine-dolosiltstones, likely due to distal storm events (Bridge and Demicco, 2008; Nichols, 2009).

#### 5. Sea-level fluctuations and evolution of depositional settings

Based on the vertical evolution of the depositional environments, the LWC section has been placed in a regional sequential framework (Fig. 3A). A T-R sequence is proposed and correlated with the second third-order Smithian sequence of Paull and Paull (1993), also documented by Vennin et al. (2015) and Olivier et al. (2016) in the southern part of the SFB. The base of the transgressive trend reflects a transition from continental to shallow marine tide-dominated red beds (Smith, 1969; corresponding to the non-described Unit A) evolving into the

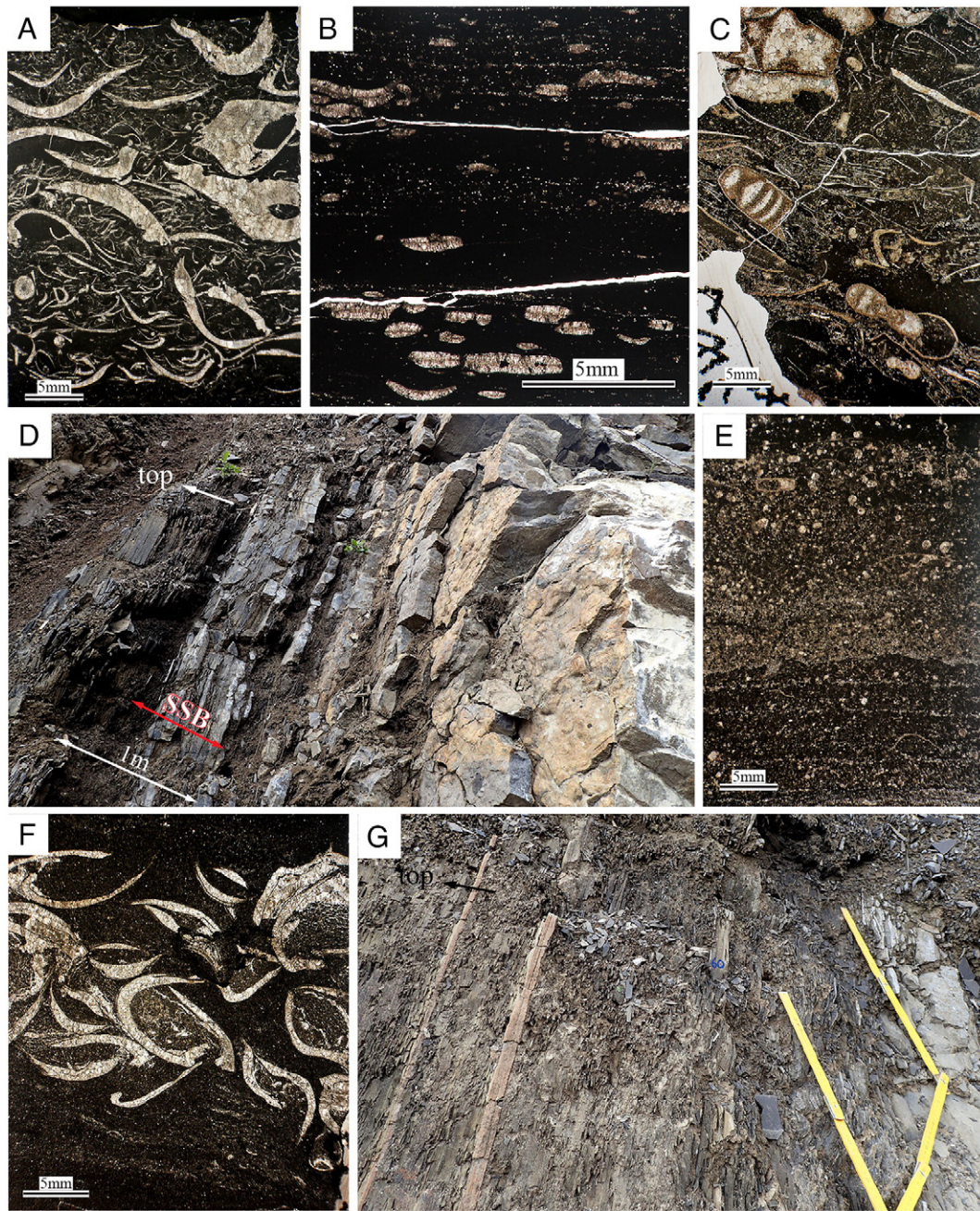


**Fig. 7.** Facies association illustrations of the storm- and mud-dominated mid ramp settings. (A) Microscopic view of the bivalve-dominated F6a. Note the bimodality in shell size locally forming umbrella structures. (B) Facies association F6b composed of disarticulated shells of bivalves, with a planar organization. (C) Microphotograph of facies association F6c characteristic of the *Anasibirites* beds. (D) Field view of the SSB above the *Anasibirites* beds intercalated within the black marl subfacies association F9b. (E) Usually observed vertical succession of facies association F7 composed of peloidal grainstone, brachiopod-gastropod grainstone, and wackestone/mudstone. (F) Microphotograph of a well-preserved articulated thick-shelled bivalve level of F8 displaying a floatstone texture where bivalves are embedded within a micritic to microsparitic matrix. (G) Field view of the classic subfacies association F9a where fine-grained dolosiltstone levels are interbedded into muds. The top of the section is indicated on field views.

siliciclastic/microbial peritidal ramp (F1 and F2 of Unit B). The transgressive episode reached its maximum above the *Anasibirites* beds corresponding to a mud-dominated mid to outer ramp domain (Unit C). The maximum flooding is indicated by the presence of deepest conditions illustrated by associated fine dolosiltstones and mudstones, and black marls (F9a and F9b, respectively). It passes to a regressive trend characterized by a transition from the mud-dominated mid to outer ramp to the tide-influenced bioclastic mid ramp evolving upward to a siliciclastic peritidal system (Unit D).

This Smithian transgression (Unit B; Fig. 3A) is marked by the appearance and development of microbial deposits (F2) in association with ca. 100 m of dolosiltstones and bioclastic calcarenites (F1)

organized in tidal megaripples. The microbial deposits are developed as MISS (Noffke et al., 2001; Noffke and Awramik, 2013; Davies et al., 2016) in a flat peritidal system (Wright, 1984; Burchette and Wright, 1992; Fig. 8). Regarding modern and ancient microbial morphologies and microstructures (Schieber et al., 2007; Noffke, 2010; Bouton et al., 2016; Davies et al., 2016), MISS recorded in the LWC section display a low diversity of morphologies (Fig. 5) in a wide range of hydrodynamic conditions (Fig. 8). MISS first occur as a cap on megaripples and are also observed at their base as wrinkle structures and laminae (F2b; Table 1, Fig. 3A). Microbial mats are commonly reworked forming chips (F2c). The chips are systematically observed at the base, top, and inside the megaripples indicating higher hydrodynamic conditions, whereas they

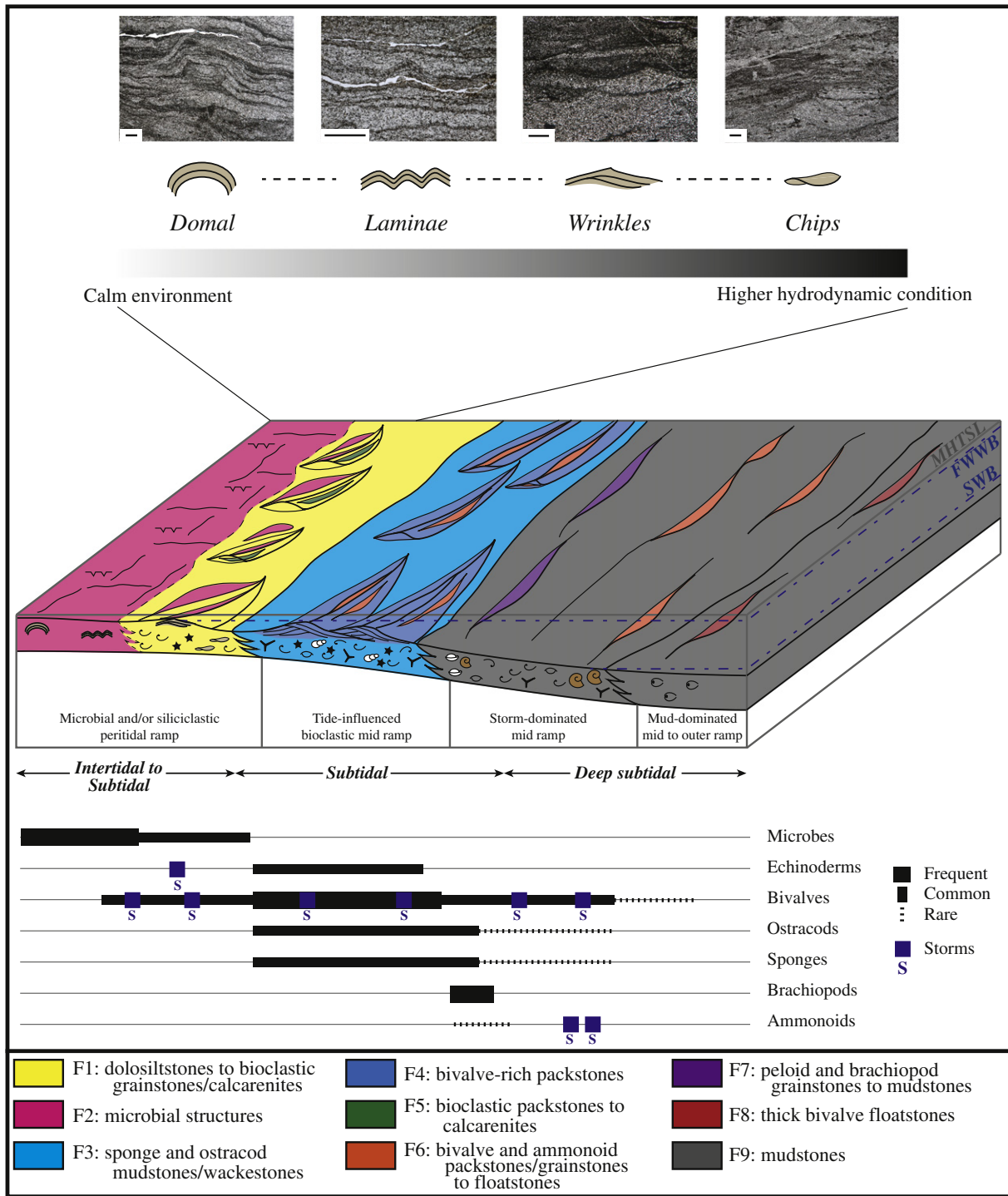


**Fig. 8.** Depositional model showing the facies association distribution through the ramp from the MISS-driven peritidal to the mud-dominated deep subtidal setting. The repartition of microbial microstructures and bioclasts is also illustrated. For the legend see Fig. 3. MHTSL: Mean High Tide Sea Level; FWWB: Fair Weather Wave Base; SWB: Storm Wave Base.

progressively disappear toward the top of Unit B, where irregular planar laminae and domes dominate along a 7 m-thick interval (Fig. 3A). The development of small cm-scale domes (F2a) implies local zones of higher water depth and/or quieter inner ramp environment, which are favourable conditions for the flourishing of microbial communities (Noffke and Awramik, 2013). The absence of reworked microbial chips confirms low hydrodynamic conditions. The cm-thick domes developed in alternation with desiccation cracks associated with wrinkle structures. Their succession indicates low amplitude variations of sea-level with an increase when domes developed. This peritidal domain is

locally affected by storm-induced events as evidenced by shell-beds composed of bivalves and gastropods (F5a and F5b) and echinoderms (F5c) (Fig. 8). The composition of the storm-induced deposits is related to the bioclastic mid ramp domain and is interpreted as washover incursions in the peritidal setting (Seilacher, 1982; Aigner, 1985; Brechley and Harper, 1998; Pruss et al., 2004).

MISS disappear concomitantly with an important increase in sea-water level as indicated by the occurrence of several ammonoid-rich layers (*Anasibirites* beds; F6c and F7; Unit C; Fig. 3A), and the deposition of mudstones (F9a) and black marls (F9b) (Fig. 8). The late Smithian

flooding event is dated by the *Anasibirites* beds and correlates throughout the whole SFB (Paull and Paull, 1993; Lucas et al., 2007; Brayard et al., 2013; Vennin et al., 2015; Olivier et al., 2016). The following early Spathian regressive trend is characterized by the progressive deposition of shell beds. The first ones are composed of in situ cm-thick bivalve-rich levels (F8). They evolve into thicker storm-induced bioclastic accumulations (F6a) organized in a shallow-upward trend. This regressive trend is also confirmed by the transition from F9 attributed to a mud-dominated mid to outer ramp, to bioclastic tidal megaripples (F4) associated laterally with sponge/ostracod wackestones (F3), and on top of Unit D to mixed siliciclastic and bioclastic tidal megaripples (F1a and F1b) developed in a peritidal domain (Fig. 8).

## 6. Factors influencing microbial development in LWC

Early Triassic microbial deposits are mostly described as microbialites in carbonate-dominated successions (Baud et al., 2007; Marengo et al., 2012; Vennin et al., 2015; Olivier et al., 2016). The facies and microfacies analysis performed in the LWC section indicates that MISS proliferated during the middle to late Smithian sedimentation. This new occurrence of microbial deposits in siliciclastic environments is older than classical wrinkle structures previously described in some Spathian deposits of the SFB (Pruss et al., 2004; Mata and Bottjer, 2011). Well-developed Smithian microbial deposits commonly occur in the southern part of the SFB but are not preserved as MISS (Brayard et al., 2011; Olivier et al., 2014, 2016; Vennin et al., 2015).

### 6.1. Sediment supply and bathymetry

The LWC section records the stacking of 111 m of dolosiliciclastic sediments from the base to the top of Unit B with apparently only minor changes in hydrodynamic conditions and sedimentary environments (Fig. 3A). Such a pattern suggests a balance between the creation of accommodation and sediment supply maintaining the water depth on the ramp (i.e., bathymetry) and allowing the aggradation of the system in a moderately hydrodynamic peritidal setting. Our results argue for the intermittent flourishing of MISS at least during the deposition of 104 m of sediments. The top of Unit B – corresponding to the Smithian–Spathian transition – is marked by an increase in accommodation as indicated by the transition from peritidal inner and mid ramp where MISS are preserved, to storm- and mud-dominated mid to outer ramp driven by a carbonate sedimentation without microbial deposits (Figs. 3 and 8). Due to the flat relief of the ramp and without evidence of a sudden tectonic movement, this important increase in sea-water level implies a rapid landward displacement of the shoreline and a destabilization of the proximal peritidal siliciclastic-microbial environments (Burchette and Wright, 1992). This drowning during the Smithian–Spathian transition clearly marks the cessation of the microbial deposits in LWC.

Recently, Vennin et al. (2015) and Olivier et al. (2016) reconstructed the depositional environments of some areas of the southern SFB during the Smithian and early Spathian, including the Minersville (MV) and Torrey (TO) sectors (Fig. 1B). In MV, microbialites mainly flourished during the Smithian transgressive trend of the large-scale third-order depositional sequence in a main inner ramp domain. Smithian microbial-bearing beds are followed by bioclastic beds deposited on a sharp surface interpreted as a medium-scale sequence boundary (Vennin et al., 2015). This surface marks an abrupt transition from a microbial peritidal system to a bioclastic tidal-influenced shoreface environment. Microbialites are observed again only during the Spathian regressive trend. In TO, the microbialite-bioclastic transition is also marked by a sequence boundary at the base of the bioclastic unit that discriminates the change from a peritidal system over a tide-dominated shoal complex (Olivier et al., 2016).

As no local synsedimentary tectonics has been well identified along the studied sedimentary succession, as well as in the southern part of the SFB (Olivier et al., 2014), relative sea-level fluctuations seem to primarily influence microbial/bioclastic substitution in the SFB. Such observations and interpretations have also been made by Bagherpour et al. (2017) on earliest Triassic microbialites (Griesbachian) from South China. They invoked an abrupt regional sea-level rise, possibly combined with the effects of regional tectonics, as a major factor involving the cessation of microbialite constructions.

### 6.2. Hydrodynamic conditions

Four types of MISS structures have been preserved in dolosiliciclastic sedimentation of Unit B in LWC (Fig. 5). Along the Smithian ramp, microbial deposits are dominated by well-preserved laminae and domal structures in protected areas of the inner domain and by wrinkles and chips associated with megaripples in a mid ramp setting (Fig. 8). This points toward a zonation of MISS morphologies in a proximal-distal transect along the ramp. Actualistic investigations highlight that – whether precipitating (microbialites/stromatolites) or not (MISS) – microbial mats better grow during quiet periods with low erosion or in environments with low hydrodynamism (Gerdes et al., 2000; Noffke et al., 2003; Cuadrado et al., 2014). Hydrodynamic conditions along the Smithian ramp in LWC seem to be moderate and relatively constant during the period of dolosiliciclastic sedimentation, likely corresponding to an “ecological window” sensu Noffke et al. (2002), where hydraulic reworking is moderate. Along the LWC ramp system, the observed bimodality in microbial structures reflects the local impact of hydrodynamism on MISS development. Without hydrodynamism in inner protected settings, microbial mats form laminae and domes that facilitate the trapping of sediments by “baffling” and the biostabilization of the substrate by grain cohesion (Gerdes et al., 2000; Noffke, 2000; Noffke et al., 2001). By contrast, when tidal currents occur in the subtidal mid ramp, microbial mats are thin at the top and at the base of tidal megaripples and are rarely stacked. Resulting MISS are commonly disrupted and reworked, forming chips. In association with megaripples, they probably developed during temporarily decantation or reduced flow regime of the tidal system or in the protected back area (Gerdes et al., 2000; Gerdes, 2007; Noffke, 2008; Stal, 2012; Cuadrado et al., 2014). In modern environments, Bouton et al. (2016) observed non-mineralized microbial mats preserved in the submersed zone of the Cayo Coco hypersaline lagoon, where low-energy conditions and decantation prevailed. This resembles our observations in LWC. Moreover, various morphologies have been also described in Triassic microbialites of MV, where Vennin et al. (2015) determined a proximal-distal zonation along the platform. They observed wavy and upper plane beds characterizing respectively lower and upper flow regimes and thin crusts in proximal intertidal settings, oncoids and contorted complex structures in higher hydrodynamic conditions in inter- to subtidal settings, and thick crusts and coalescent domes in distal subtidal environments where lower flow regime prevailed. These modern and ancient cases highlight that hydrodynamism influences calcified and non-calcified microbial deposits and controls the described proximal-distal distribution of MISS in LWC. Our observations on LWC MISS thus support hydrodynamism as one of their main controlling parameters, as also documented for calcified microbial mats associated with Early Triassic peritidal environments (Kershaw et al., 1999; Baud et al., 2007; Woods and Baud, 2008; Vennin et al., 2015).

### 6.3. Is the apparent absence of carbonate precipitation at LWC linked to substrate lithology?

According to Pruss et al. (2004), the occurrence of wrinkle structures in Spathian shallow subtidal siliciclastic environments is unusual as microbial deposits are preferably preserved in carbonate systems

(Schubert and Bottjer, 1992; Lehrmann et al., 2015). Our results show the development of MISS in subtidal and intertidal dolosiliclastic environments at least since the middle Smithian suggesting that such deposits were probably not so rare in Early Triassic environments. MISS are identified in marine and terrestrial siliciclastic (paleo)environments where they formed 2D structures by binding and trapping of sediment particles without precipitation of calcium carbonate (Gerdes et al., 2000; Schieber et al., 2007; Noffke, 2009; Noffke and Awramik, 2013; Davies et al., 2016). Due to the phototrophic requirement of autotrophic cyanobacteria, mats can develop well in fine quartz sands, which efficiently enable the conduction of solar radiation in translucent grains (Gerdes et al., 1985; Noffke et al., 2001). Nevertheless, many microbial mats are neither systematically direct actors of carbonate precipitation nor are they able to precipitate carbonate when environmental physico-chemical conditions change (Arp et al., 2003; Dupraz et al., 2009). Some studies have also reported uncommon early precipitation of CaCO<sub>3</sub> in microbial mats in peculiar siliciclastic settings (Druschke et al., 2008; Kremer et al., 2008; Cuadrado et al., 2011). These different studies suggest that the siliciclastic composition of the substratum alone does not explain the apparent absence of microbial-mediated precipitation as observed in LWC. Indeed, the composition of microbial communities, as well as the physico-chemical characteristics of the water column and substratum, are likely prime factors influencing the mineralization of microbial mats in siliciclastic environments.

Based on the worldwide geographic variations of Early Triassic calcified microbial deposits, Kershaw et al. (2012) and Kershaw (2017) suggested that, over global perturbations (such as carbon cycle or climate fluctuations), physico-chemical conditions (CaCO<sub>3</sub> saturation, upwellings and water surface circulation) may have had an important impact on microbial mat flourishing, morphologies and precipitation. It is well known that the precipitation of CaCO<sub>3</sub> in microbial mats can be constrained by the alkalinity of sea-waters (Arp et al., 2001, 2003; Dupraz et al., 2009). Biogenic calcification is often favoured when waters are supersaturated in CaCO<sub>3</sub> (Pentecost and Riding, 1986; Riding, 2000; Riding et al., 2014). The apparent absence of bio-precipitation in the north of the SFB during the ?Griesbachian–Smithian, where MISS are preserved in siliciclastic sediments (this work; Wimer, 2015), clearly contrasts with the south SFB where microbialites developed in a carbonate setting (e.g., MV section; Vennin et al., 2015). Recent geochemical studies show that beyond the water chemistry, differential early diagenetic processes at the water-sediment interface likely took place within the SFB, e.g., inducing authigenic carbonate precipitation in some places (Thomazo et al., 2016; Caravaca et al., 2017b). The northern part of the SFB may have also been probably more influenced by terrigenous influxes than the southern part (Caravaca et al., 2017b). This may have prevented the mineralization of microbial mats at LWC. A simpler hypothesis is that microbial communities present at LWC may have not possessed the capacity to mineralize. Overall, these observations suggest that local physico-chemical conditions, rather than global events, may have primarily controlled the spatial, temporal and morphological development of microbial mats in the SFB during the Early Triassic.

## 7. Conclusions

The facies analysis of the sedimentary succession preserved at the Lower Weber Canyon site provides new evidence regarding microbial flourishing during the Early Triassic and the local and regional factors controlling their development. Nine facies associations are recognized and distributed along the LWC section in depositional settings ranging from microbial/dolosiliclastic peritidal ramp, tide-influenced bioclastic mid ramp, storm-dominated mid ramp, to mud-dominated mid to outer ramp. In the absence of bio-induced carbonate precipitation, microbial deposits are interpreted as MISS that flourished in a mainly peritidal setting where hydrodynamic conditions influenced their morphological disparity. Four microbial structures developed in

two main distinct depositional settings. On the one hand, wrinkles and chips dominate the microbial assemblage in tide-influenced mid ramp characterized by bioclastic and dolosiliclastic megariipples affected by some storm-induced events. On the other hand, laminae and domal structures are preferably recorded in protected areas behind megariipples or in inner ramp where subaerial exposure commonly occurred.

The vertical stacking of at least 100 m of dolosilstones where MISS developed during the Smithian transgression argues for sufficient available space for sedimentation maintaining a stable bathymetry favourable for microbial development. The Smithian transgressive interval allowed microbial mats to flourish from north to south in the SFB. Nevertheless, our results suggest that the fine quartz composition of the substrate is not the only factor favouring the development of MISS. Indeed, local physico-chemical conditions of the peritidal dolosiliclastic environment (CaCO<sub>3</sub> water saturation, intensity of terrigenous fluxes, or early diagenesis) did not provide ideal conditions for calcification of microbial mats or for their preservation. Moreover, as some microbial mat communities do not contribute to carbonate precipitation, the composition of the living microbial community can be questioned at LWC.

The late Smithian sediments record the deepening of the depositional environment by transgression inducing a migration of the depositional setting toward a carbonate-dominated ramp accompanied by the cessation of microbial deposits, or at least by the end of their preservation. Then, bivalve shells accumulated either in tidal megariipples or in proximal tempestites interbedded with sponge/ostracod muds in the bioclastic mid ramp, while ammonoid beds, distal tempestites, black marls and fine muddy/silty deposits record the opening of the depositional environment to storm- and mud-dominated mid to outer ramp systems.

Therefore, this study of Smithian MISS represents a new step in the understanding of Early Triassic microbial deposits, their geographical repartition, as well as their morphological variability. Based on their high disparity, we suggest that local factors have significant impacts on the development of microbial structures, rather than global factors such as ocean anoxia or climate. Further regional investigations are now needed to better disentangle the processes influencing the spatial and temporal development of microbial deposits and their relationships with other biotic communities during the Early Triassic.

## Acknowledgements

This study benefited from the financial supports of the ANR project AFTER (ANR-13-JS06-0001-01) and of the FEDER Bourgogne Franche-Comté. We thank private land owners (Scott Rees – south side of Weber River and Mrs. Monte Brough – north side of Weber River) for allowing access to their lands. We also thank S. Bourquin and an anonymous reviewer for constructive comments that helped to improve the manuscript.

## References

- Aigner, T., 1982. Calcareous tempestites: storm-dominated stratification in Upper Muschelkalk limestones (Middle Trias, SW-Germany). In: Einsele, G., Seilacher, A. (Eds.), *Cyclic and Event in Stratification*. Springer, Berlin, pp. 180–198.
- Aigner, T., 1985. Storm depositional systems. *Lecture Notes in Earth Sciences* 3, 1–158.
- Arp, G., Reimer, A., Reitner, J., 2001. Photosynthesis-induced biofilm calcification and calcium concentrations in Phanerozoic oceans. *Science* 292, 1701–1704.
- Arp, G., Reimer, A., Reitner, J., 2003. Microbialite formation in seawater of increased alkalinity, Satonda Crater Lake, Indonesia. *Journal of Sedimentary Research* 73, 105–127.
- Bagherpour, B., Bucher, H., Baud, A., Brosse, M., Vennemann, T., Martini, R., Guodun, K., 2017. Onset, development, and cessation of basal Early Triassic microbialites (BETM) in the Nanpanjiang pull-apart Basin, South China Block. *Gondwana Research* 44, 178–204.
- Baud, A., Cirilli, S., Marcoux, J., 1997. Biotic response to mass extinction: the lowermost Triassic microbialites. *Facies* 36, 238–242.
- Baud, A., Richoz, S., Pruss, S.B., 2007. The Lower Triassic anachronistic carbonate facies in space and time. *Globol and Planetary Change* 55, 81–89.
- Blakey, R.C., 1977. Petroliferous lithosomes in the Moenkopi Formation, Southern Utah. *Geology* 4, 67–84.

- Bouton, A., Vennin, E., Pace, A., Bourillot, R., Dupraz, C., Thomazo, C., Brayard, A., Désaubliaux, G., Visscher, P.T., 2016. External controls on the distribution, fabrics and mineralization of modern microbial mats in a coastal hypersaline lagoon, Cayo Coco (Cuba). *Sedimentology* 63, 972–1016.
- Boyer, D.L., Bottjer, D.J., Droser, M.L., 2004. Ecological signature of Lower Triassic shell beds of the Western United States. *Palaios* 19, 372–380.
- Brayard, A., Brühwiler, T., Bucher, H., Jenks, J., 2009. *Guodunites*, a low-palaeolatitude and trans-Panthalassic Smithian (Early Triassic) ammonoid genus. *Palaeontology* 52, 471–481.
- Brayard, A., Vennin, E., Olivier, N., Bylund, K.G., Jenks, J.F., Stephen, D.A., Bucher, H., Hofmann, R., Goudemand, N., Escarguel, G., 2011. Transient metazoan reefs in the aftermath of the end-Permian mass extinction. *Nature Geoscience* 4, 693–697.
- Brayard, A., Bylund, K.G., Jenks, J.F., Stephen, D.A., Olivier, N., Escarguel, G., Fara, E., Vennin, E., 2013. Smithian ammonoid faunas from Utah: implications for Early Triassic biostratigraphy, correlations and basal paleogeography. *Swiss Journal of Palaeontology* 132, 141–219.
- Brayard, A., Meier, M., Escarguel, G., Fara, E., Nützel, A., Olivier, N., Bylund, K.G., Jenks, J.F., Stephen, D.A., Hautmann, M., Vennin, E., Bucher, H., 2015. Early Triassic Gulliver gastropods: spatio-temporal distribution and significance for biotic recovery after the end-Permian mass extinction. *Earth-Science Reviews* 146, 31–64.
- Brayard, A., Krumenacker, L.J., Bottjer, J.P., Jenks, J.F., Bylund, K.G., Fara, E., Vennin, E., Olivier, N., Goudemand, N., Saucède, T., Charbonnier, S., Romano, C., Doguzhaeva, L., Thuy, B., Hautmann, M., Stephen, D.A., Thomazo, C., Escarguel, G., 2017. Unexpected Early Triassic marine ecosystem and the rise of the modern evolutionary fauna. *Science Advances*:3 <https://doi.org/10.1126/sciadv.1602159>.
- Brenchley, P.J., Harper, D.A.T., 1998. *Palaeoecology: Ecosystems, Environments and Evolution*. Chapman & Hall, London (402 pp.).
- Brett, C.E., Seilacher, A., Einsele, G., 1991. Fossil-Lagerstätten: a taphonomic consequence of event sedimentation. In: Ricken, W., Seilacher, A. (Eds.), *Cycles and Events in Stratigraphy*. Springer-Verlag, New York, pp. 283–297.
- Bridge, J.S.S., Demicco, R.V., 2008. *Earth Surface Processes, Landforms and Sediment Deposits*. Cambridge University Press, New York (815 pp.).
- Burchette, T.P., Wright, V.P., 1992. Carbonate ramp depositional systems. *Sedimentary Geology* 79, 3–57.
- Burchfiel, B., Davis, G.A., 1975. Nature and controls of Cordilleran orogenesis, Western United States: extensions of an earlier synthesis. *American Journal of Science* 275, 363–396.
- Burne, R.V., Moore, L.S., 1987. Microbialites: organosedimentary deposits of benthic microbial communities. *Palaios* 2, 241–254.
- Caravaca, G., Brayard, A., Vennin, E., Guiraud, M., Le Pourhiet, L., Grosjean, A.-S., Thomazo, C., Olivier, N., Fara, E., Escarguel, G., Bylund, K.G., Jenks, J.F., Stephen, D.A., 2017a. Controlling factors for differential subsidence in the Sonoma Foreland Basin (Early Triassic, western USA). *Geological Magazine* <https://doi.org/10.1017/S0016756817000164>.
- Caravaca, G., Thomazo, C., Vennin, E., Olivier, N., Coquerez, T., Escarguel, G., Fara, E., Jenks, J.F., Bylund, K.G., Stephen, D.A., Brayard, A., 2017b. Early Triassic fluctuations of the global carbon cycle: new evidence from paired carbon isotopes in the western USA basin. *Global and Planetary Change* 154, 10–22.
- Carr, T.R., Paull, R.K., 1983. Early Triassic stratigraphy and paleogeography of the Cordilleran miogeoclinal. In: Reynolds, A., Dolly, E.D. (Eds.), *Mesozoic Paleogeography of the West-Central United States*. SEPM Rocky Mountain Section, Symposium Vol. 2, pp. 39–55.
- Clark, D.L., 1957. Marine Triassic stratigraphy in eastern Great Basin. *AAPG Bulletin* 41, 2102–2222.
- Collinson, J.W., Hasenmuller, W.A., 1978. Early Triassic paleogeography and biostratigraphy of the Cordilleran miogeosyncline. In: Howell, D.G., McDougall, K.A. (Eds.), *Mesozoic Paleogeography of the Western United States*. SEPM Pacific Section, Los Angeles, pp. 175–187.
- Collinson, J.W., Kendall, C.G.S.C., Marcantel, J.B., 1976. Permian-Triassic boundary in eastern Nevada and west-central Utah. *Geological Society of America Bulletin* 87, 821–824.
- Cuadrado, D.G., Carmona, N.B., Bournod, C., 2011. Biostabilization of sediments by microbial mats in a temperate siliciclastic tidal flat, Bahía Blanca estuary (Argentina). *Sedimentary Geology* 237, 95–101.
- Cuadrado, D.G., Perillo, G.M.E., Vitale, A.J., 2014. Modern microbial mats in siliciclastic tidal flats: evolution, structure and the role of hydrodynamics. *Marine Geology* 352, 367–380.
- Davies, N.S., Liu, A.G., Gibling, M.R., Miller, R.F., 2016. Resolving MISS conceptions and misconceptions: a geological approach to sedimentary surface textures generated by microbial and abiotic processes. *Earth-Science Reviews* 154, 210–246.
- Dickinson, W.R., 2013. Phanerozoic palinspatic reconstructions of the Great Basin geotectonics (Nevada-Utah, USA). *Geosphere* 9, 1384–1396.
- Druschke, P.A., Jiang, G., Anderson, T.B., Hanson, A.D., 2008. Stromatolites in the Late Ordovician Eureka Quartzite: implications for microbial growth and preservation in siliciclastic settings. *Sedimentology* 56, 1275–1291.
- Dupraz, C., Reid, R.P., Braissant, O., Decho, A.W., Norman, R.S., Visscher, P.T., 2009. Processes of carbonate precipitation in modern microbial mats. *Earth-Science Reviews* 96, 141–162.
- Embry, A.F., 1997. Global sequence boundaries of the Triassic and their identification on the Western Canada sedimentary basin. *Bulletin of Canadian Petroleum Geology* 45, 415–433.
- Flügel, E., 2002. Triassic reef patterns. In: Kiessling, W., Flügel, E., Golonka, J. (Eds.), *Phanerozoic Reef Patterns*. SEPM vol. 72, pp. 391–463.
- Flügel, E., 2004. *Microfacies of Carbonate Rocks*. Springer, Berlin (976 pp.).
- Forel, M.-B., Crasquin, S., Kershaw, S., Collin, P.-Y., 2013. In the aftermath of the end-Permian extinction: the microbialite refuge? *Terra Nova* 25, 137–143.
- Fürsich, F.T., Oschmann, W., 1993. Shell beds as tools in basin analysis: the Jurassic of Kachchh, western India. *Journal of the Geological Society* 150, 169–185.
- Galfetti, T., Bucher, H., Brayard, A., Hochuli, P.A., Weissert, H., Guodun, K., Atudorei, V., Guex, J., 2007. Late Early Triassic climate change: insights from carbonate carbon isotopes, sedimentary evolution and ammonoid paleobiogeography. *Palaeogeography Palaeoclimatology Palaeoecology* 243, 394–411.
- Gerdes, G., 2007. Structures left by modern microbial mats in their host sediments. In: Schieber, J., Bose, P.K., Eriksson, P.G., Banerjee, S., Sarkar, S., Altermann, W., Catuneanu, O. (Eds.), *Atlas of Microbial Mat Features Preserved within the Siliciclastic Rock Record*. *Atlases in Geoscience* vol. 2, pp. 5–38.
- Gerdes, G., 2010. What are Microbial Mats? In: Seckbach, J., Oren, A. (Eds.), *Microbial Mats: Modern and Ancient Microorganisms in Stratified Systems*. *Cellular Origin, Life in Extreme Habitats and Astrobiology* 14, pp. 3–25.
- Gerdes, G., Krumbein, W.E., 1994. Peritidal potential stromatolites – a synopsis. In: Bertrand-Sarfati, J., Monty, C. (Eds.), *Phanerozoic Stromatolites II*. Springer, Dordrecht, pp. 101–129.
- Gerdes, G., Krubbein, W.E., Reineck, H.E., 1985. The depositional record of sandy, versicolored tidal flats (Mellum Island, southern North Sea). *Journal of Sedimentary Research* 55, 265–278.
- Gerdes, G., Claes, M., Dunajtschik-Piewak, K., Riege, H., Krumbein, W.E., Reineck, H.E., 1993. Contribution of microbial mats to sedimentary surface structures. *Facies* 29, 61–74.
- Gerdes, G., Klenke, T., Noffke, N., 2000. Microbial signatures in peritidal siliciclastic sediments: a catalogue. *Sedimentology* 47, 279–308.
- Goodspeed, T.H., Lucas, S.G., 2007. Stratigraphy, sedimentology, and sequence stratigraphy of the Lower Triassic Sinbad Formation, San Raphael Swell, Utah. *New Mexico Museum of Natural History & Science Bulletin* 40, 91–101.
- Grasby, S.E., Beauchamp, B., Embry, A., Sanei, H., 2013. Recurrent Early Triassic ocean anoxia. *Geology* 41, 175–178.
- Haq, B.U., Hardenbol, J., Vail, P.R., 1987. Chronology of fluctuating sea levels since the Triassic 250 million years ago to present. *Science* 235, 1135–1167.
- Hofmann, R., Hautmann, M., Brayard, A., Nützel, A., Bylund, K.G., Jenks, J.F., Vennin, E., Olivier, N., Bucher, H., 2014. Recovery of benthic marine communities from the end-Permian mass extinction at the low latitudes of Eastern Panthalassa. *Palaeontology* 57, 547–589.
- Hose, R.K., Repenning, C.A., 1959. Stratigraphy of Pennsylvanian, Permian, and Lower Triassic rocks of Confusion Range, west-central Utah. *AAPG Bulletin* 43, 2167–2196.
- Ingersoll, R.V., 2008. Subduction-Related Sedimentary Basins of the USA Cordillera. In: Miall, A.D. (Ed.), *The Sedimentary Basins of the United States and Canada*. *Sedimentary Basins of the World* vol. 5, pp. 395–428.
- Jattiot, R., Bucher, H., Brayard, A., Monnet, C., Jenks, J.F., Hautmann, M., 2016. Revision of the genus *Anasibirites* Mojsisovics (Ammonoidea): an iconic and cosmopolitan taxon of the late Smithian (Early Triassic) extinction. *Papers in Palaeontology* 2, 155–188.
- Jattiot, R., Bucher, H., Brayard, A., Brosse, M., Jenks, J.F., Bylund, K.G., 2017. Smithian ammonoid faunas from northeastern Nevada: implications for Early Triassic biostratigraphy and correlation within the western USA basin. *Palaeontographica A (Paleozoology, Stratigraphy)* 309, 1–89.
- Johnson, H.D., Baldwin, C.T., 1996. Shallow clastic seas. In: Reading, H.G. (Ed.), *Sedimentary Environments: Processes, Facies and Stratigraphy*, Third edition Blackwell, Oxford, pp. 232–280.
- Kershaw, S., 2017. Palaeogeographic variation on the Permian–Triassic boundary microbialites: a discussion of microbial and ocean processes after the end-Permian mass extinction. *Journal of Palaeogeography* 6, 97–107.
- Kershaw, S., Zhang, T., Lan, G., 1999. A ?microbialite carbonate crust at the Permian-Triassic boundary in South China, and its palaeoenvironmental significance. *Palaeogeography, Palaeoclimatology, Palaeoecology* 146, 1–18.
- Kershaw, S., Crasquin, S., Forel, M.-B., Randon, C., Collin, P.-Y., Reynolds, A., Guo, L., 2010. Earliest Triassic microbialites in Cürük Dag, southern Turkey; composition, sequences and controls on formation. *Sedimentology* 58, 739–755.
- Kershaw, S., Crasquin, S., Li, Y., Collin, P.-Y., Forel, M.-B., Mu, X., Baud, A., Wang, Y., Xie, S., Maurer, F., Guo, L., 2012. Microbialites and global environmental change across the Permian-Triassic boundary: a synthesis. *Geobiology* 10, 25–47.
- Kidwell, S.M., Bosence, D.W.J., 1991. Taphonomy and time-averaging of marine shelly faunas. In: Allison, P.A., Briggs, D.E.G. (Eds.), *Releasing the Data Locked in the Fossil Record*. *Topics in Geobiology* vol. 9, pp. 115–209.
- Kidwell, S.M., Fürsich, F.T., Aigner, T., 1986. Conceptual framework for the analysis and classification of fossil concentrations. *Palaios* 1, 228–238.
- Kremer, B., Kazmierczak, J., Stal, L.J., 2008. Calcium carbonate precipitation in cyanobacterial mats from sandy tidal flats of the North Sea. *Geobiology* 6, 46–56.
- Lehrmann, D.J., Bentz, J.M., Wood, T., Goers, A., Dhillon, R., Akin, S., Li, X., Payne, J.L., Kelley, B.M., Meyer, K.M., Schaal, E.K., Suarez, M.B., Yu, M., Qin, Y., Li, R., Minzoni, M., Henderson, C.M., 2015. Environmental controls on the genesis of marine microbialites and dissolution surface associated with the end-Permian mass extinction: new sections and observations from the Nanpanjiang basin, south China. *Palaios* 30, 529–552.
- Lucas, S.G., Krainer, K., Milner, A.R.C., 2007. The type section and age of the Timpoweap Member and stratigraphic nomenclature of the Triassic Moenkopi Group in the south-western Utah. In: Lucas, S.G., Spielmann, J.A. (Eds.), *Triassic of the American West*. *New Mexico Museum of Natural History and Science Bulletin* vol. 40, pp. 109–118.
- Marenco, P.J., Griffin, J.M., Fraiser, M.L., Clapham, M.E., 2012. Paleogeology and geochemistry of Early Triassic (Spathian) microbial mounds and implications for anoxia following the end-Permian mass extinction. *Geology* 40, 715–718.
- Mata, S.A., Bottjer, D.J., 2009. The paleoenvironmental distribution of Phanerozoic wrinkle structures. *Earth-Science Reviews* 96, 181–195.
- Mata, S.A., Bottjer, D.J., 2011. Origin of Lower Triassic microbialites in mixed carbonate-siliciclastic successions: ichnology, applied stratigraphy, and the end-Permian mass extinction. *Palaeogeography, Palaeoclimatology, Palaeoecology* 300, 158–178.
- Mata, S.A., Bottjer, D.J., 2012. Microbes and mass extinctions: paleoenvironmental distribution of microbialites during times of biotic crisis. *Geobiology* 10, 3–24.
- McKee, E.D., 1954. Stratigraphic history of the Moenkopi Formation of Triassic age. *Geological Society of America Memoirs* 61, 1–133.
- Monaco, P., 2000. Biological and physical agents of shell concentrations of *Lithotites* facies enhanced by microstratigraphy and taphonomy, Early Jurassic, Trento area (Northern Italy). *GeoResearch Forum* 6, 473–486.
- Newell, N.D., 1948. Key Permian section, Confusion Range, Western Utah. *Geological Society of America Bulletin* 59, 1027–1052.

- Nichols, G., 2009. *Sedimentology and Stratigraphy*. Second edition. Wiley-Blackwell, Oxford (419 pp.).
- Noffke, N., 2000. Extensive microbial mats and their influences on the erosional and depositional dynamics of a siliciclastic cold water environment (Lower Arenigian, Montagne Noire, France). *Sedimentary Geology* 136, 207–215.
- Noffke, N., 2008. Turbulent lifestyle: microbial mats on Earth's sandy beaches—today and 3 billion years ago. *GSA Today* 18. <https://doi.org/10.1130/GSATG7A.1>.
- Noffke, N., 2009. The criteria for the biogenicity of microbially induced sedimentary structures (MISS) in Archean and younger, sandy deposits. *Earth-Science Reviews* 96, 173–180.
- Noffke, N., 2010. *Microbial Mats in Sandy Deposits from the Archean Era to Today*. Springer, Heidelberg (194 pp.).
- Noffke, N., Awramik, S.M., 2013. Stromatolites and MISS – differences between relatives. *GSA Today* 23, 4–9.
- Noffke, N., Gerdes, G., Klenke, T., Krumbein, W.E., 2001. Microbially induced sedimentary structures – a new category within the classification of primary sedimentary structures. *Journal of Sedimentary Research* 71, 649–656.
- Noffke, N., Knoll, A.H., Grotzinger, J.P., 2002. Ecology and taphonomy of microbial mats in late neoproterozoic siliciclastics: a case study from the Nama Group, Namibia. *Palaios* 17, 1–12.
- Noffke, N., Gerdes, G., Klenke, T., 2003. Benthic cyanobacteria and their influence on sedimentary dynamics of peritidal depositional systems (siliciclastic, evaporitic salty, and evaporitic carbonatic). *Earth-Science Reviews* 62, 163–176.
- Olivier, N., Brayard, A., Fara, E., Bylund, K.G., Jenks, J.F., Vennin, E., Stephen, D.A., Escarguel, G., 2014. Smithian shoreline migrations and depositional settings in Timpoweap Canyon (Early Triassic, Utah, USA). *Geological Magazine* 5, 938–955.
- Olivier, N., Brayard, A., Vennin, E., Escarguel, G., Fara, E., Bylund, K.G., Jenks, J.F., Caravaca, G., Stephen, D.A., 2016. Evolution of depositional settings of the Torrey area during the Smithian (Early Triassic, Utah, USA) and their significance for the biotic recovery. *Geological Journal* 51, 600–626.
- Paull, R.A., Paull, R.K., 1993. Interpretation of Early Triassic nonmarine–marine relations, Utah, USA. In: Lucas, S.G., Morales, M. (Eds.), *The Nonmarine Triassic*. New Mexico Museum of Natural History and Science Bulletin vol. 3, pp. 403–409.
- Payne, J.L., Lehrmann, D.J., Christensen, S., Wei, J., Knoll, A.H., 2006. Environmental and biological controls on the initiation and growth of a Middle Triassic (Anisian) reef complex on the Great Bank of Guizhou, Guizhou Province, China. *Palaios* 21, 325–343.
- Pentecost, A., Riding, R., 1986. Calcification in cyanobacteria. In: Leadbeater, B.S.C., Riding, R. (Eds.), *Biomining in Lower Plants and Animal*. Systematics Association Special vol. 30, pp. 73–90.
- Pflüger, F., Gresse, P.G., 1996. Microbial sand chips – a non-actualistic sedimentary structure. *Sedimentary Geology* 102, 263–274.
- Pruss, S., Fraiser, M., Bottjer, D.J., 2004. Proliferation of Early Triassic wrinkle structures: implications for environmental stress following the end-Permian mass extinction. *Geology* 32, 461–464.
- Reineck, H.E., Gerdes, G., Claes, M., Dunajtschik, K., Riege, H., Krumbein, W.E., 1990. Microbial modification of sedimentary surface structures. In: Heling, D., Rothe, P., Förstner, U., Stoffers, P. (Eds.), *Sediments and Environmental Geochemistry*. Springer, Berlin, pp. 254–276.
- Riding, R., 2000. Microbial carbonates: the geological record of calcified bacterial–algal mats and biofilms. *Sedimentology* 47, 179–214.
- Riding, R., Liang, L., Braga, J.C., 2014. Millennial-scale ocean acidification and late quaternary decline of cryptic bacterial crusts in tropical reefs. *Geobiology* 12, 387–405.
- Schieber, J., 1999. Microbial mats in terrigenous clastics; the challenge of identification in the rock record. *Palaios* 14, 3–12.
- Schieber, J., Bose, P.K., Eriksson, P.G., Banerjee, S., Sarkar, S., Altermann, W., Catuneanu, O., 2007. *Atlas of Microbial Mat Features Preserved within the Siliciclastic Rock Record*. *Atlases in Geoscience 2*. Elsevier, Amsterdam (311 pp.).
- Schubert, J.K., Bottjer, D.J., 1992. Early Triassic stromatolites as post-mass extinction disaster forms. *Geology* 20, 883–886.
- Seilacher, A., 1982. Distinctive features of sandy tempestites. In: Einsele, G., Seilacher, A. (Eds.), *Cyclic and Event in Stratification*. Springer, Berlin, pp. 333–349.
- Seilacher, A., Reif, W.-E., Westphal, F., Riding, R., Clarkson, E.N.K., Whittington, H.B., 1985. Sedimentological, ecological and temporal patterns of fossil Lagerstätten. *Philosophical Transactions of the Royal Society of London B311*, 5–23.
- Smith, H.P., 1969. *The Thaynes Formation of the Moenkopi Group North-Central Utah*. (Ph.D. Thesis). University of Utah, USA (168 pp.).
- Stal, L.J., 2012. Cyanobacterial mats and stromatolites. In: Whittom, B.E. (Ed.), *Ecology of Cyanobacteria II. Their Diversity in Space and Time*. Springer, Berlin, pp. 65–126.
- Sun, Y., Joachimski, M.M., Wignall, P.B., Yan, C., Chen, Y., Jiang, H., Wang, L., Li, X., 2012. Lethally hot temperatures during the Early Triassic greenhouse. *Science* 338, 366–370.
- Szulc, J., 2007. Sponge-microbial stromatolites and coral-sponge reef recovery in the Triassic of the western Tethys domain. In: Lucas, S.G., Spielmann, J.A. (Eds.), *The Global Triassic*. New Mexico Museum of Natural History and Science Bulletin vol. 41, p. 402.
- Tang, H., Kershaw, S., Liu, H., Tan, X., Li, F., Hu, G., Huang, C., Wang, L., Lian, C., Li, L., Yang, X., 2017. Permian–Triassic boundary microbialites (PTBMs) in southwest China: implications for palaeoenvironment reconstruction. *Facies* 63. <https://doi.org/10.1007/s10347-016-0482-8>.
- Thomazo, C., Vennin, E., Brayard, A., Bour, I., Mathieu, O., Elmeknassi, S., Olivier, N., Escarguel, G., Bylund, K.G., Jenks, J., Stephen, D.A., Fara, E., 2016. A diagenetic control on the Early Triassic Smithian–Spathian carbon isotopic excursions recorded in the marine settings of the Thaynes Group (Utah, USA). *Geobiology* 14, 220–236.
- Tucker, M.E., 1985. Shallow-marine carbonate facies and facies model. In: Brenchley, P.J., Williams, B.P.J. (Eds.), *Sedimentology Recent Developments and Applied Aspects*. Geological Society of London Special Publication vol. 18, pp. 147–169.
- Vennin, E., Olivier, N., Brayard, A., Bour, I., Thomazo, C., Escarguel, G., Fara, E., Bylund, K.G., Jenks, J.F., Stephen, D.A., Hofmann, R., 2015. Microbial deposits in the aftermath of the end-Permian mass extinction: a diverging case from the Mineral Mountains (Utah, USA). *Sedimentology* 62, 753–792.
- Werhmann, A., Gerdes, G., Höfling, R., 2012. Microbial mats in a Lower Triassic siliciclastic playa environment (middle Buntsandstein, North Sea). In: Noffke, N., Chafetz, H. (Eds.), *Microbial Mats in Siliciclastic Depositional Systems through Time*. SEPM Special Publication vol. 101, pp. 177–190.
- Wimer, E., 2015. *Microbially Induced Sedimentary Structures as an Ecological Niche in Subtidal Early Triassic Environments of Eastern Panthalassa*. (McS Thesis). University of Wisconsin-Milwaukee, USA (72 pp.).
- Woods, A.D., 2014. Assessing Early Triassic paleoceanographic conditions via unusual sedimentary fabrics and features. *Earth-Science Reviews* 137, 6–18.
- Woods, A.D., Baud, A., 2008. Anachronistic facies from a drowned Lower Triassic carbonate platform: lower member of the Alwa Formation (Ba'id Exotic), Oman Mountains. *Sedimentary Geology* 209, 1–14.
- Wright, V.P., 1984. Peritidal carbonate facies models: a review. *Geological Journal* 19, 309–325.
- Wright, V.P., Burchette, T.P., 1996. Shallow-water carbonate environments. In: Reading, H.G. (Ed.), *Sedimentary Environments: Processes, Facies and Stratigraphy*. Blackwell, Oxford (UK), pp. 325–392.